



Title	Study on Mediator as a regulator of heterochromatin assembly
Author(s)	大屋, 恵梨子
Citation	北海道大学. 博士(理学) 甲第11091号
Issue Date	2013-09-25
DOI	10.14943/doctoral.k11091
Doc URL	http://hdl.handle.net/2115/53917
Type	theses (doctoral)
File Information	Eriko_Oya.pdf



[Instructions for use](#)

Study on Mediator as a regulator of heterochromatin assembly

(ヘテロクロマチン形成の制御因子としてのメディエーターに関する研究)

Eriko Oya

Dissertation

Department of Chemistry, Graduate School of Science,

Hokkaido University

2013

Index

I. Introduction	5
I-i. Heterochromatin and Epigenetics	
I-ii. Heterochromatin assembly in fission yeast	
I-iii. RNAi dependent heterochromatin formation	
I-iv. Rrp6 dependent heterochromatin formation	
I-v. Mediator	
I-vi. Purpose of this study	
II. Experimental procedure	12
II-i. Strains and culture media	
II-ii. Silencing assays	
II-iii. Chromatin immunoprecipitation (ChIP) analysis	
II-iv. RNA preparation using hot phenol method	
II-v. Northern Blotting	
II-vi. siRNA analysis	
II-vii. RT-PCR	
II-viii. qPCR	
II-ix. ChIP-qPCR and RT-PCR using synchronized <i>cdc25-22</i> cells	
II-x. Microarray analysis of Mediator mutants	
II-xi. Stability assay of variegation phenotypes	
Table 1. Strains used in this study	
Table S2. Primers used in this study	
III. Results	20
III-i. Mediator is required for heterochromatic silencing at the pericentromeres.	
III-i-a. Loss of Mediator causes defects in heterochromatin-dependent gene silencing.	
III-i-b. Loss of Mediator shows variegated phenotype.	
III-i-c. Loss of Mediator causes the accumulation of transcripts from pericentromeric region.	
III-i-d. Conclusion	

- III-ii. Mediator localizes with RNAPII at the pericentromeric repeats.
 - III-ii-a. Mediator localizes pericentromeric heterochromatin with RNAPII in cell cycle dependent manner.
 - III-ii-b. Conclusion
- III-iii. Loss of Med18 or Med20 causes defects in heterochromatin structure at the pericentromeres.
 - III-iii-a. Loss of Med18/20 causes defects in heterochromatin structure at the pericentromeres.
 - III-iii-b. Conclusion
- III-iv. Med18 is required for Rrp6-dependent H3K9 methylation at the pericentromere.
 - III-iv-a. Med18 functions in a pathway distinct from the RNAi-dependent pathway.
 - III-iv-b. Med18 is required for Rrp6-dependent H3K9 methylation at the pericentromere.
 - III-iv-c. Mediator might functions in a step after association of Rrp6 on chromatin for heterochromatin formation.
 - III-iv-d. Conclusion
- III-v. Mediator is required for the generation of siRNA from pericentromeric ncRNA.
 - III-v-a. Med18/Mediator is also involved in the RNAi-dependent heterochromatin pathway.
 - III-v-b. Mediator is required for siRNA formation at the pericentromeric repeats.
 - III-v-c. Conclusion
- III-vi. Mediator promotes efficient siRNA formation from RITS-bound ncRNA.
 - III-vi-a. Mediator is not required for the step of the association of the RITS complex and RDRC to heterochromatin.
 - III-vi-b. Mediator plays a role in the step following the binding of the RITS complex to target RNA.
 - III-vi-c. Conclusion
- III-vii. Mediator is required for efficient transcription in heterochromatin.
 - III-vii-a. Mutation of Mediator would not be expected to affect mating locus heterochromatin.

III-vii-b.	Mediator is required for efficient transcription in heterochromatin.	
III-vii-c.	Med18 negatively regulates transcription in the compromised heterochromatin.	
III-vii-d.	Conclusion	
III-viii.	Effect of Mediator disruption on euchromatic genes	
III-viii-a.	The effect of <i>med18Δ</i> and <i>med20Δ</i> on euchromatic gene expression.	
III-viii-b.	Some euchromatic genes, including stress response genes, might be repressed by the RNAi/Mediator system.	
III-viii-c.	Conclusion	
IV.	Discussion	49
IV-i.	IV-i Efficient siRNA production is required for effective spreading.	
IV-ii.	MHD functions after RITS associates with heterochromatic repeats and/or target RNA.	
IV-iii.	Mediator acts in a step after the association of Rrp6/exosome with chromatin.	
IV-iv.	Mediator is required for transcriptional activation in heterochromatin.	
IV-v.	Mediator is required for transcriptional activation in heterochromatin.	
IV-vi.	Conclusion	
V.	References	59
VI.	Acknowledgement	64

I. Introduction

I-i. Chromatin and Epigenetics

In eukaryotic cells, genomic DNA is folded with histone and non-histone proteins to form chromatin. Recent analysis revealed that chromatin structure directly regulates epigenetic change of gene expression in the various biological activities such as development and the response to environmental stimuli. In addition, the chromatin structure is determined by chemical modifications on histone. The modifications function as a signal platform to recruit effectors/readers, which ultimately determine the chromatin structure and the following meaningful biological outcome. Chromatin is found in two varieties on the basis of differential compaction at interphase: euchromatin and heterochromatin (Figure 1).

Euchromatin is less condensed, more accessible and generally more easily transcribed by RNA polymerase II (RNAPII). In these loci, the histones are acetylated on lysine residues mainly in the N-terminal tail region. In particular, it is believed that the presence of acetylated lysine and methylated lysine 4 on the histone tails acts as a general marker for euchromatin.

On the other hand, heterochromatin is typically highly condensed, inaccessible and highly ordered in nucleosomal arrays. There are two types of heterochromatin, constitutive and facultative heterochromatin. Constitutive heterochromatin is found at the chromosomal regions that contain a high density of repetitive DNA element such as clusters of satellite sequences and transposable elements. These regions, which are found at centromeres and telomeres, remain condensed throughout the cell cycle. Facultative heterochromatin is found at developmentally regulated loci, where the chromatin state can change in response to cellular signals and gene activity.

Heterochromatin plays an important role in gene regulation and the maintenance of genome integrity. A key feature of heterochromatin is its ability to spread in *cis*, causing epigenetic silencing. In female mammalian X-chromosome inactivation, heterochromatin spreads from a specific nucleation site, causing silencing of most of the X chromosome, thereby regulating gene dosage.

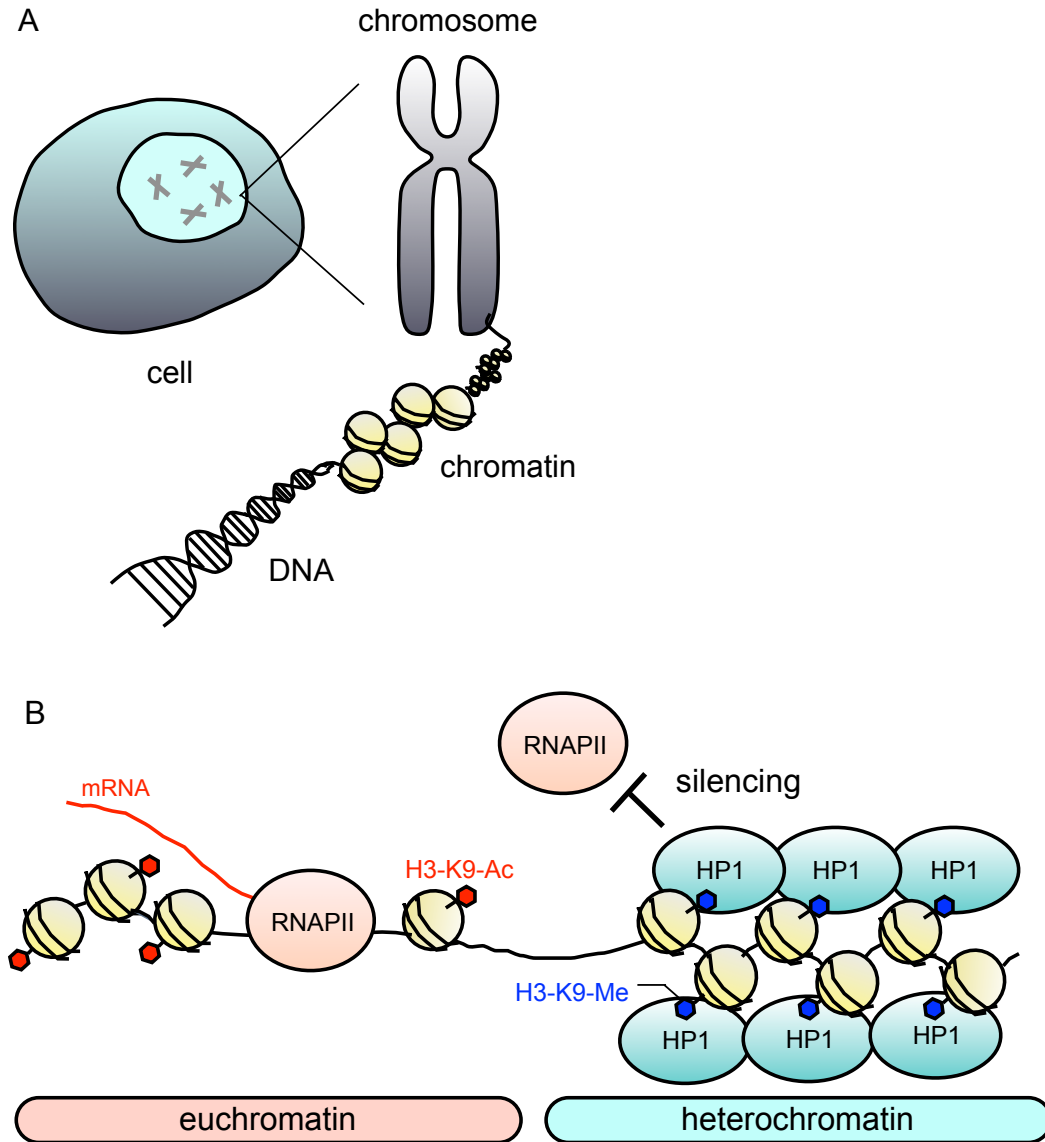


Figure 1. Chromatin Structure

- (A) In eukaryotic cells, genomic DNA is folded with histone and non-histone proteins to form chromatin.
- (B) Chromatin is found in two varieties on the basis of differential compaction at interphase: euchromatin and heterochromatin. Euchromatin is less condensed, more accessible and generally more easily transcribed. In these loci, the histones are acetylated on lysine residues in the N-terminal tail and on the surface of the nucleosome core. Heterochromatin is typically highly condensed, inaccessible and highly ordered in nucleosomal arrays. These regions are rich in methylation of histone H3K9 (H3K9me), which is critical for the binding of HP1 proteins.

Heterochromatin is also associated with various genome functions such as, chromosomal segregation, suppression of recombination and repression of selfish elements.

I-ii. Heterochromatin assembly in fission yeast

The fission yeast *Schizosaccharomyces pombe* provides a good model system for investigating heterochromatin formation because it is a unicellular eukaryote suitable for genetic analysis, and its heterochromatin structure and RNAi machinery resemble those in metazoa. In fission yeast, heterochromatin is preferentially formed across large chromosomal domains at the pericentromeres, subtelomeres and the mating-type locus. These regions are rich in methylation of histone H3K9 (H3K9me), which is catalyzed by the histone methyltransferase Clr4, a homolog of mammalian SUV39h [1, 2]. The modification of H3K9me is critical for the binding of HP1 proteins [2, 3], which recruit various factors for the assembly of repressive chromatin and associated various functions [4, 5].

I-iii. RNAi dependent heterochromatin formation

Several distinct pathways promote heterochromatin assembly in fission yeast. At the pericentromere, RNAi machinery plays essential roles in heterochromatin formation [6, 7]. Pericentromeric heterochromatin is assembled on the outer repeat (*otr*) region (containing of *dg* and *dh* repeats), and the outer portion of the innermost repeats (*imr*), which surround the central core (*cnt*) domain, the site of kinetochore assembly (Figure 2) [8]. The repeats are transcribed by RNA polymerase II (RNAPII) to produce non-coding RNAs (ncRNAs) during S-phase [9-11]. Transcribed ncRNAs give rise to double strand RNA via the RNA-dependent RNA polymerase complex (RDRC), comprised of Rdp1, Cid12 and Hrr1, and are processed into small interfering RNA (siRNA) by the RNase III helicase Dicer (Dcr1). The siRNAs are then loaded into an RNA-induced transcriptional silencing (RITS) complex composed of Ago1, Tas3 and Chp1 [7]. siRNAs target the RITS complex to cognate nascent transcripts, resulting in the recruitment of additional factors, including RDRC and ultimately Clr4, to methylate histone H3K9. Generation of siRNA and heterochromatin assembly are interdependent processes that form a self-enforcing

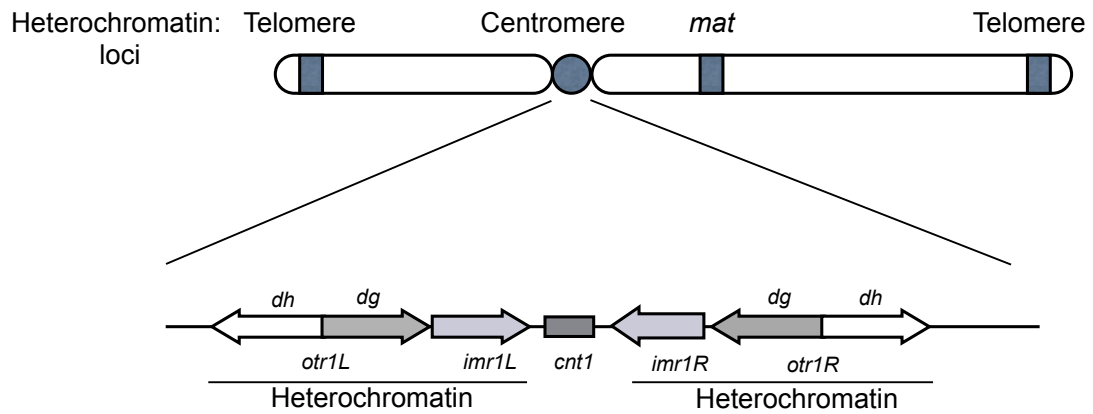


Figure 2. The main heterochromatic region in fission yeast.

Schematic of heterochromatic loci observed at pericentromeres, subtermeres and mating locus in fission yeast. Pericentromeric heterochromatin is assembled on the outer repeat (*otr*) region (containing of *dg* and *dh* repeats), and the outer portion of the innermost repeats (*imr*), which surround the central core (*cnt*) domain, the site of kinetochore assembly.

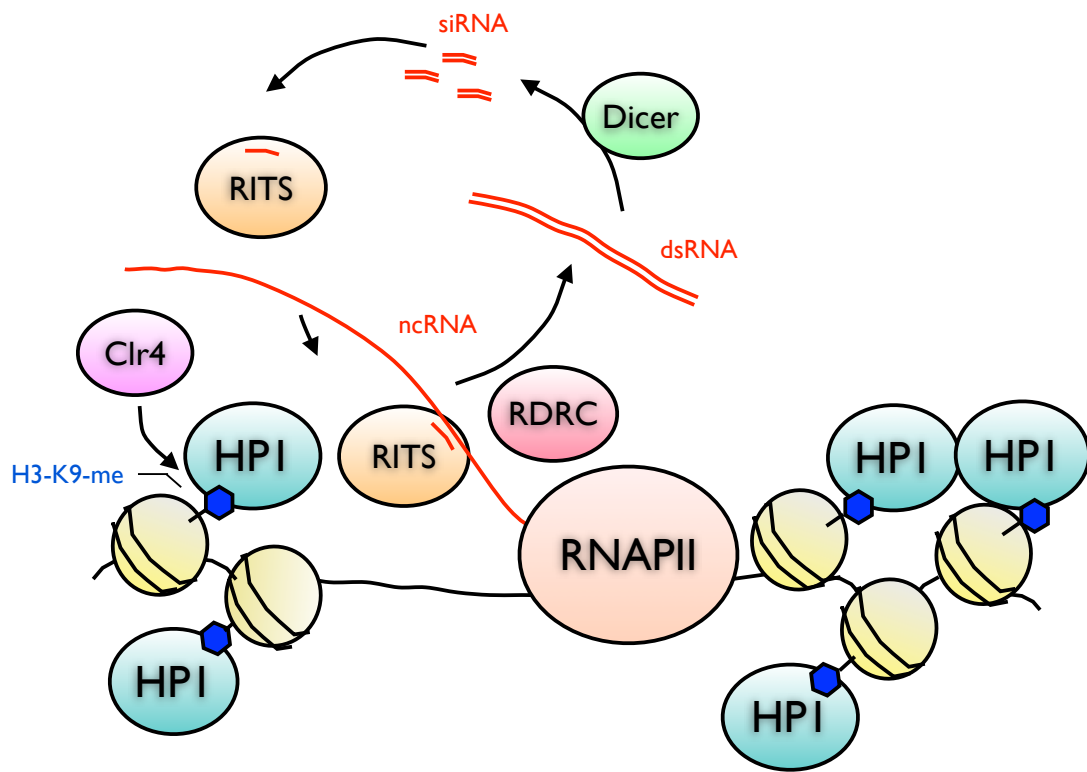


Figure 3. RNAi dependent heterochromatin formation

The pericentromeric repeats are transcribed by RNA polymerase II (RNAPII) to produce non-coding RNAs (ncRNAs) during S-phase. Transcribed ncRNAs give rise to double strand RNA via the RNA-dependent RNA polymerase complex (RDRC), comprised of Rdp1, Cid12 and Hrr1, and are processed into small interfering RNA (siRNA) by the RNase III helicase Dicer (Dcr1). The siRNAs are then loaded into an RNA-induced transcriptional silencing (RITS) complex composed of Ago1, Tas3 and Chp1. siRNAs target the RITS complex to cognate nascent transcripts, resulting in the recruitment of additional factors, including RDRC and ultimately Clr4, to methylate histone H3K9. Generation of siRNA and heterochromatin assembly are interdependent processes that form a self-enforcing loop.

loop (Figure 3) [12, 13]. Importantly, RNAPII appears to couple transcription at the target loci to the generation of siRNAs. This was shown by the fact that a specific mutation in RNAPII results in a decrease in heterochromatic histone modifications, accumulation of pericentromeric transcripts, and accompanying loss of siRNA, which are effects that were observed previously in RNAi mutants [10].

Heterochromatin, once established, spreads into neighboring region, which is typically shown by the heterochromatin formation and silencing of the genes inserted into heterochromatin. This process depends on RNAi system and probably couples with transcription [14, 15].

I-iv. Rrp6 dependent heterochromatin formation

Nuclear RNA is monitored by a nuclear RNA surveillance system involving exosomes with 3'-5' exonuclease activity, and a portion of the ncRNA at the pericentromere has been shown to be degraded by the nuclear exosome [16, 17]. In addition to RNA degradation, 3'-5' exonuclease Rrp6, a component of the nuclear exosome, was shown to mediate heterochromatin formation in parallel with RNAi, which is demonstrated by the cumulative increase and decrease of H3K9me at the pericentromere in the double null-mutant of *ago1* and *rrp6* [18]. Since the amount of siRNA is not affected by depletion of Rrp6, Rrp6-dependent heterochromatin formation occurs via a pathway that is distinct from that of RNAi-dependent siRNA generation [16]. The molecular basis of the Rrp6-dependent pathway is not yet clear.

I-v. Mediator

Mediator, which is a well-conserved protein complex consisting of at least 20 subunits, was first identified as a factor that mediates DNA transcription factors binding at regulatory sequences and RNAPII at promoters for the efficient start of transcription [19, 20] and has been shown to be required for transcription of almost all protein-coding genes *in vivo* [21-23]. Structural analysis indicates that this complex consists of four distinct structural domains: head, middle, tail and kinase. The head domain is responsible for extensive interaction with RNAPII, and the Med18/Pmc6-Med20 heterodimer, which is a portion of the head domain, binds to the core head domain through the C-terminal helix of Med8 [24]. The head domain stabilizes the

connection between RNAPII and TFIIF, which facilitates the transition of RNAPII from initiation complex to elongation complex [25]. In addition to the promotion of general transcription from protein-coding genes, recent studies have revealed a new function of Mediator. In *Arabidopsis thaliana*, Mediator directs the transcription of ncRNA genes by recruiting RNAPII to their promoters [26]. In mammalian cells, a specific subunit of Mediator functions as an interaction site for alternative mRNA splicing or transcription elongation factors [27, 28]. These data suggest that this subunit of Mediator might play roles in both transcription elongation and the subsequent processing of transcripts as a platform for the binding of various factors.

I-vi. Purpose of this study

Since both Rrp6-dependent heterochromatin formation and RNAi-dependent heterochromatin formation are coupled to transcription, we assumed that the factor(s) that interacts with RNAPII directs the coupling. Therefore, we assessed the role of several RNAPII-interacting factors including Mediator in pericentromeric heterochromatin assembly. We found that the disruption of non-essential subunits of the Mediator head domain, Med18 and Med20, compromised both RNAi-dependent and Rrp6-dependent heterochromatin assembly at the pericentromere. In addition, the head domain is required for transcriptional activation in heterochromatin. Therefore, we propose that Mediator links transcription and processing of ncRNA by RNAi and exosomes for the formation of centromeric heterochromatin.

II. Experimental procedure

III-ii. Strains and culture media

The *S. pombe* strains used in this study are described in Table S1. The media and genetic methods used in the study were essentially as described previously [29]. Yeast cells were cultured in YES at 30°C. For deletion or epitope-tagging of the target genes, the PCR-based module method [30] was used.

III-iii. Silencing assays

Silencing assays were conducted from overnight unsaturated cultures grown in 10 ml YES. A 5-fold dilution series of cells was spotted on N/S plates (YES in all spot figures, except Figure 5A and 13C), 5-FOA plates (N/S plates with the addition of 1 g/l 5-fluoroorotic acid), and Low Ade plates (N/S plates including limited amount of adenine). The plates were then incubated at 30°C for 3 days.

III-iv. Chromatin immunoprecipitation (ChIP) analysis

Cells (2.5×10^8) growing exponentially in YES were fixed with 1% formaldehyde (Nacalai Tesque) for 30 min at 25°C. After quenching the fixation with 150 mM glycine, cells were harvested and washed twice with Buffer 1 (50 mM HEPES (pH 7.5), 140 mM NaCl, 1 mM EDTA, 1% TritonX-100, and 0.1% Na-deoxycholate). The cell pellet was re-suspended in Buffer 1 containing a protease inhibitor cocktail (1:20; Nacalai Tesque) and homogenized with a bead shocker (Yasui kikai). The cell extract was made up to 2 ml with Buffer 1 containing protease inhibitor cocktail (1:100) and sonicated for 240 seconds with a New Biorupter (CosmoBio) set at level “H”. After sonication, the cell extract was centrifuged at 15,000 rpm for 15 min. The input fraction was used for immunoprecipitation with secondary antibody-conjugated magnetic beads (DYNAL). Anti-myc (4A6/Millipore), anti-FLAG (M2/Sigma), anti-H3K9me2 (a gift from T. Urano, Shimane University) and anti-Swi6 (produced in-house) were used as the primary antibodies. Magnetic beads (50 μ l) were incubated with 1.5 g of primary antibody for 1 h at 4°C before incubating with the cell extracts. After immunoprecipitation, the beads were washed with Buffer 1, followed by two

washes each with Buffer 1' (50 mM HEPES (pH 7.5), 500 mM NaCl, 1 mM EDTA, 1% TritonX-100, and 0.1% Na-deoxycholate), Buffer 2 (10 mM Tris (pH 8.0), 250 mM LiCl, 0.5% NP-40, and 0.5% Na-deoxycholate) and TE buffer (10 mM Tris (pH 8.0), 1 mM EDTA). Beads were resuspended in 100 µg/ml RNase A containing TE buffer incubated for 10 min at 37°C. Then, Proteinase K (0.5 mg/ml) was added and the mixture digested for a further 1 h at 42°C. After de-cross-linking, DNA was purified using a QIAquick PCR purification kit (Qiagen). qPCR was performed as described above. The primers used for ChIP analysis are listed in Table S2.

III-v. RNA preparation using hot phenol method

Total RNA was isolated from logarithmically-growing *S. pombe* (in YES media) using the hot phenol method[31]. Cells were grown to mid-log phase in YES medium at 30°C. Cells (1×10^8). The cells were harvested by centrifugation and resuspended in 400 µl of 50 mM Na acetate pH5.3, 10mM EDTA ('AE buffer'). The resuspended cells were transferred to a 1.5 ml microcentrifuge tube and 40 µl of 10% SDS was added. The suspension was vortexed and an equal volume of fresh phenol, previously equilibrated with AE buffer, was added. The mixture was again vortexed and incubated at 65°C for 4min. The mixture was then rapidly chilled in a dry ice/ethanol bath until phenol crystals appeared, and then centrifuged for 2 min at maximum speed in microcentrifuge to separate the aqueous and phenol phases. The upper, aqueous phase was transferred to a fresh microcentrifuge tube and extracted with phenol/chloroform at room temperature for 5 min. The extracted aqueous phase was then brought to 0.3M Na acetate, pH5.3, by adding 40 µl of 3M Na acetate pH5.3, after which 2.5 volumes of ethanol were added to precipitate the RNA. After washing with 80% ethanol, the pellet was dried and resuspended in 20 µl sterile water and stored at -80°C until used. Throughout the preparation, normal precautions to avoid ribonuclease contamination were taken.

III-vi. Northern Blotting

Total RNA was isolated from logarithmically-growing *S. pombe* (in YES media) using the hot phenol method. For northern blotting of centromeric and mat RNA, 50 mg of total RNA was electrophoresed on a 1% agarose gel containing 1× MOPS and

1% formaldehyde. RNA was transferred to positively-charged nylon membranes (Amersham Biosciences) in 10× SSC by standard capillary blotting. Following UV crosslinking of the RNA to the nylon filter, prehybridization and hybridization were carried out at 42°C in UltraHyb-Oligo buffer (Ambion). For hybridization, 50 pmol oligos were end-labeled with [γ 32 P]dATP (3000Ci/mmol) using T4 Polynucleotide Kinase (TOYOBO). After hybridization for 24 h, membranes were washed four times in 2× SSC/0.1% SDS for 10 min at 42°C before exposure to an imaging plate for 1–2 days. For re-probing, probes on the membrane were stripped by boiling in 200 ml of 0.5× SSC/0.1% with shaking. Oligonucleotides used as probes are shown in Table S2.

III-vii. siRNA analysis

Small RNA fractions were prepared from 1×10^9 cells grown exponentially in YES liquid medium using the mirVana miRNA Isolation Kit (Ambion). Small RNA (15 g) was resuspended in 50% formamide containing a dye and separated on a 15% urea-denaturing poly-acrylamide gel. Samples on the gel were blotted onto a Hybond-N membrane (Amersham Biosciences) using a Trans-Blot SD semi-dry electrophoretic transfer cell (BioRad). Oligonucleotide probes labeled with 32 P complimentary to *dh*, *dg*, *ura4*, *ade6* or *tRNA* were generated using T4 polynucleotide kinase (TOYOBO) according to the manufactures instructions. Probes used for detecting siRNA were hybridized to the membrane for 48 h at 42°C in a rotating oven. After hybridization, the membrane was washed with 2×SSC buffer containing 2% SDS for 30 min and then with 0.5×SSC buffer containing 0.1% SDS for 30 min at 42°C. The imaging plate was exposed for 1–3 days. All oligonucleotides used as probes are listed in Table S2.

III-viii. RT-PCR

For RT-PCR analysis, total RNA was cleaned up and treated with Recombinant DNase I (RNase-free) (TaKaRa) according to the manufacturer's instructions. RT-PCR was performed using PrimeScript Reverse Transcriptase (TaKaRa) according to the manufacturer's instructions. Primer sequences are shown in Table S2.

III-ix. **qPCR**

qPCR was performed using SYBR premix Ex-Taq (TaKaRa) and the Thermal Cycler Dice Real time system TP800 (TaKaRa). Primer sequences are shown in Table S2.

III-x. **ChIP-qPCR and RT-PCR using synchronized *cdc25-22* cells**

cdc25-22 cells were grown at 25°C to a concentration of 2×10^6 cells/ml and then shifted to 36°C for 4 hr and 15 min to stop the cell cycle at the G2/M phase. Samples for ChIP assay were collected every 30 min for 300 min after shifting the cells back to 25°C to release cell cycle block. ChIP assay was performed as described in the Experimental Procedures. To prepare RNA for RT-PCR, the input fractions of ChIP were adjusted to 0.25% SDS and 0.25 mg/ml proteinase K and incubated for 45 min at 45°C and then at 65°C for more than 4 hours to reverse crosslinking. Samples were extracted once with phenol-chloroform. After ethanol precipitation, the samples were resuspended in a suitable volume of DEPC-treated distilled water. RT-PCR was performed as described in the Experimental Procedures.

III-xi. **Microarray analysis of Mediator mutants**

Microarray analysis for gene expression was performed as described previously [32] using FY2002 as a parental strain. White and pink epiclones of *med18Δ* and *med20Δ* were analyzed separately. The sequences of the probes and original data from the microarray experiments were deposited to GEO (<http://www.ncbi.nlm.nih.gov/geo/index.cgi> with accession number GSE43543).

III-xii. **Stability assay of variegation phenotypes**

White or pink epiclones on Low Ade plates (YES plates including limited amount of adenine) were cultured for several generations in complete medium. Aliquots were taken from the cultures before and after the cultivation, appropriately diluted, and then plated onto Low Ade plates and incubated at 30°C for several days to allow white or pink colonies to form. Conversion rates were calculated using the following formula: conversion rate = $1 - (F/I)^{1/N}$, where F is the final percentage of white or pink colonies, I is the initial percentage of white or pink colonies, and N is the number

of generations between I and F [33, 34].

Table 1. Strains used in this study

<u>Name</u>	<u>Genotype</u>	<u>Source</u>
FY2002	<i>h⁺, leu1-32, ade6-DN/N, ura4-DS/E, imr1L::ura4⁺, otr1R::ade6⁺</i>	R. Allshire
HKV-324	<i>h⁺, leu1-32, ade6-DN/N, ura4-DS/E, imr1L::ura4⁺, otr1R::ade6⁺, clr4Δ::kanMX6</i>	our stock
HKV-325	<i>h⁺, leu1-32, ade6-DN/N, ura4-DS/E, imr1L::ura4⁺, otr1R::ade6⁺, dcr1Δ::kanMX6</i>	our stock
HKV-435	<i>h⁺, leu1-32, ade6-DN/N, ura4-DS/E, imr1L::ura4⁺, otr1R::ade6⁺, med1Δ::kanMX6</i>	this study
HKV-389	<i>h⁺, leu1-32, ade6-DN/N, ura4-DS/E, imr1L::ura4⁺, otr1R::ade6⁺, med27Δ::kanMX6</i>	this study
HKV-391	<i>h⁺, leu1-32, ade6-DN/N, ura4-DS/E, imr1L::ura4⁺, otr1R::ade6⁺, med18Δ::kanMX6</i>	this study
EOS-164	<i>h⁺, leu1-32, ade6-DN/N, ura4-DS/E, imr1L::ura4⁺, otr1R::ade6⁺, med20Δ::kanMX6</i>	this study
HKV-393	<i>h⁺, leu1-32, ade6-DN/N, ura4-DS/E, imr1L::ura4⁺, otr1R::ade6⁺, med19Δ::kanMX6</i>	this study
HKV-395	<i>h⁺, leu1-32, ade6-DN/N, ura4-DS/E, imr1L::ura4⁺, otr1R::ade6⁺, med12Δ::kanMX6</i>	this study
HKV-397	<i>h⁺, leu1-32, ade6-DN/N, ura4-DS/E, imr1L::ura4⁺, otr1R::ade6⁺, med13Δ::kanMX6</i>	this study
HKV-399	<i>h⁺, leu1-32, ade6-DN/N, ura4-DS/E, imr1L::ura4⁺, otr1R::ade6⁺, cdk8Δ::kanMX6</i>	this study
EOS-071	<i>h⁺, leu1-32, ade6-DN/N, ura4-DS/E, imr1L::ura4⁺, otr1R::ade6⁺, med18Δ::kanMX6 (white epiclone)</i>	this study
EOS-073	<i>h⁺, leu1-32, ade6-DN/N, ura4-DS/E, imr1L::ura4⁺, otr1R::ade6⁺, med18Δ::kanMX6 (pink epiclone)</i>	this study
EOS-205	<i>h⁺, leu1-32, ade6-DN/N, ura4-DS/E, imr1L::ura4⁺, otr1R::ade6⁺, med20Δ::kanMX6 (white epiclone)</i>	this study
EOS-206	<i>h⁺, leu1-32, ade6-DN/N, ura4-DS/E, imr1L::ura4⁺, otr1R::ade6⁺, med20Δ::kanMX6 (pink epiclone)</i>	this study
SPY797	<i>h⁺, leu1-32, ade6-m210, ura4-DS/E, otr1R(SphI)::ura4⁺, Nat-Ago1promoter-3×FLAG::ago1</i>	D. Moazed
KKS-690	<i>h⁺, leu1-32, ade6-m210, ura4-DS/E, otr1R(SphI)::ura4⁺, Nat-Ago1promoter-3×FLAG::ago1, clr4Δ::hphMX6</i>	our stock
KKS-688	<i>h⁺, leu1-32, ade6-m210, ura4-DS/E, otr1R(SphI)::ura4⁺, Nat-Ago1promoter-3×FLAG::ago1, dcr1Δ::hphMX6</i>	our stock
EOS-624	<i>h⁺, leu1-32, ade6-m210, ura4-DS/E, otr1R(SphI)::ura4⁺, Nat-Ago1promoter-3×FLAG::ago1, med18Δ::kanMX6</i>	this study
FY648	<i>h⁺, leu1-32, ade6-m210, ura4-DS/E, otr1R(SphI)::ura4⁺</i>	R. Allshire
KKS-341	<i>h⁺, leu1-32, ade6-DN/N, ura4-DS/E, imr1L::ura4⁺, otr1R::ade6⁺, chp1-13myc-kanMX6</i>	our stock
EOS-654	<i>h⁺, leu1-32, ade6-DN/N, ura4-DS/E, imr1L::ura4⁺, otr1R::ade6⁺, chp1-13myc-kanMX6, clr4Δ::hphMX6</i>	this study
EOS-656	<i>h⁺, leu1-32, ade6-DN/N, ura4-DS/E, imr1L::ura4⁺, otr1R::ade6⁺, chp1-13myc-kanMX6, dcr1Δ::hphMX6</i>	this study
EOS-650	<i>h⁺, leu1-32, ade6-DN/N, ura4-DS/E, imr1L::ura4⁺, otr1R::ade6⁺, chp1-13myc-kanMX6, med18Δ::natMX6 (white epiclone)</i>	this study
EOS-652	<i>h⁺, leu1-32, ade6-DN/N, ura4-DS/E, imr1L::ura4⁺, otr1R::ade6⁺, chp1-13myc-kanMX6, med18Δ::natMX6 (pink epiclone)</i>	this study
KKS-357	<i>h⁺, leu1-32, ade6-DN/N, ura4-DS/E, imr1L::ura4⁺, otr1R::ade6⁺, rdp1-5FLAG-natMX6</i>	our stock
EOS-660	<i>h⁺, leu1-32, ade6-DN/N, ura4-DS/E, imr1L::ura4⁺, otr1R::ade6⁺, rdp1-5FLAG-natMX6, clr4Δ::hphMX6</i>	this study
EOS-662	<i>h⁺, leu1-32, ade6-DN/N, ura4-DS/E, imr1L::ura4⁺, otr1R::ade6⁺, rdp1-5FLAG-natMX6, dcr1Δ::hphMX6</i>	this study
EOS-700	<i>h⁺, leu1-32, ade6-DN/N, ura4-DS/E, imr1L::ura4⁺, otr1R::ade6⁺, rdp1-5FLAG-natMX6, med18Δ::hphMX6 (white epiclone)</i>	this study
EOS-702	<i>h⁺, leu1-32, ade6-DN/N, ura4-DS/E, imr1L::ura4⁺, otr1R::ade6⁺, rdp1-5FLAG-natMX6, med18Δ::hphMX6 (pink epiclone)</i>	this study
SPY440	<i>h⁻, ura4-5BoxB-hphMX6</i>	D. Moazed
SPY452	<i>h⁻, ura4-5BoxB-hphMX6, tas3-λN-kanMX6</i>	D. Moazed
EOS-469	<i>h⁻, ura4-5BoxB-hphMX6, tas3-λN-kanMX6, FOA^r</i>	this study
SPY463	<i>h⁻, ura4-5BoxB-hphMX6, tas3-λN-kanMX6, clr4Δ::natMX6</i>	D. Moazed
EOS-544	<i>h⁻, ura4-5BoxB-hphMX6, tas3-λN-kanMX6, med18Δ::natMX6</i>	this study
EOS-541	<i>h⁻, ura4-5BoxB-hphMX6, tas3-λN-kanMX6, med20Δ::natMX6</i>	this study
HKV-174	<i>h⁹⁰, his2, leu1-32, ura4-DS/E, ade6-m210, kint2::ura4⁺</i>	our stock
HKV-171	<i>h⁹⁰, his2, leu1-32, ura4-DS/E, ade6-m210, kint2::ura4⁺, clr4Δ::kanMX6</i>	our stock
HKV-320	<i>h⁹⁰, his2, leu1-32, ura4-DS/E, ade6-m210, kint2::ura4⁺, dcr1Δ::kanMX6</i>	our stock
EOS-391	<i>h⁹⁰, his2, leu1-32, ura4-DS/E, ade6-m210, kint2::ura4⁺, med18Δ::kanMX6</i>	this study
EOS-643	<i>h⁹⁰, his2, leu1-32, ura4-DS/E, ade6-m210, kint2::ura4⁺, med18Δ::kanMX6, dcr1Δ::hphMX6</i>	this study
EOS-012	<i>h⁻</i>	this study
GAS-28	<i>h⁻, clr4Δ::kanMX6</i>	our stock
EOS-426	<i>h⁻, ade6-DN/N, ura4-DS/E, imr1L::ura4⁺, otr1R::ade6⁺, med18Δ::hphMX6, dcr1Δ::kanMX6</i>	this study
EOS-695	<i>h⁹⁰, his2, leu1-32, ura4-DS/E, ade6-m210, kint2::ura4⁺, rrp6Δ::natMX6</i>	this study
EOS-694	<i>h⁹⁰, his2, leu1-32, ura4-DS/E, ade6-m210, kint2::ura4⁺, dcr1Δ::kanMX6, rrp6Δ::natMX6</i>	this study
EOS-704	<i>h⁹⁰, his2, leu1-32, ura4-DS/E, ade6-m210, kint2::ura4⁺, med18Δ::kanMX6, rrp6Δ::natMX6</i>	this study
EOS-706	<i>h⁹⁰, his2, leu1-32, ura4-DS/E, ade6-m210, kint2::ura4⁺, med18Δ::kanMX6, dcr1Δ::hphMX6, rrp6Δ::natMX6</i>	this study
HKM-1374	<i>h⁺, leu1-32, ade6-DN/N, ura4-DS/E, imr1L::ura4⁺, otr1R::ade6⁺, clr4Δ::kanMX6, med8-K9</i>	this study
EOS-599	<i>h⁺, leu1-32, ade6-DN/N, ura4-DS/E, imr1L::ura4⁺, otr1R::ade6⁺, med8-K9 (white epiclone)</i>	this study
EOS-601	<i>h⁺, leu1-32, ade6-DN/N, ura4-DS/E, imr1L::ura4⁺, otr1R::ade6⁺, med8-K9 (pink epiclone)</i>	this study
HKM-1369	<i>h⁺, leu1-32, ade6-DN/N, ura4-DS/E, imr1L::ura4⁺, otr1R::ade6⁺, med31-H1</i>	this study

EOS-586	<i>h⁺, leu1-32, ade6-DN/N, ura4-DS/E, imr1L::ura4⁺, otr1R::ade6⁺, med31-H1</i> (white epiclone)	this study
EOS-588	<i>h⁺, leu1-32, ade6-DN/N, ura4-DS/E, imr1L::ura4⁺, otr1R::ade6⁺, med31-H1</i> (pink epiclone)	this study
ss216	<i>h⁺, leu1-32, ade6-DN/N, ura4-DS/E, imr1L::ura4⁺, otr1R::ade6⁺, rrp6-13myc-natMX6, dcr1Δ::hphMX6</i>	Our stock
EOS-747	<i>h⁺, leu1-32, ade6-DN/N, ura4-DS/E, imr1L::ura4⁺, otr1R::ade6⁺, rrp6-13myc-natMX6, clr4Δ::kanMX6</i>	this study
EOS-739	<i>h⁺, leu1-32, ade6-DN/N, ura4-DS/E, imr1L::ura4⁺, otr1R::ade6⁺, rrp6-13myc-natMX6, dcr1Δ::hphMX6</i>	this study
EOS-788	<i>h⁺, leu1-32, ade6-DN/N, ura4-DS/E, imr1L::ura4⁺, otr1R::ade6⁺, rrp6-13myc-natMX6, med18Δ::hphMX6</i> (white epiclone)	this study
EOS-789	<i>h⁺, leu1-32, ade6-DN/N, ura4-DS/E, imr1L::ura4⁺, otr1R::ade6⁺, rrp6-13myc-natMX6, med18Δ::hphMX6</i> (pink epiclone)	this study
EOS-797	<i>h⁺, leu1-32, ade6-DN/N, ura4-DS/E, imr1L::ura4⁺, otr1R::ade6⁺, rrp6-13myc-natMX6, dcr1Δ::hphMX6, med18Δ::hphMX6</i>	this study
EOS-588	<i>h⁺, leu1-32, ade6-DN/N, ura4-DS/E, imr1L::ura4⁺, otr1R::ade6⁺, med31-H1</i> (pink epiclone)	this study

Table S2. Primers used in this study

<u>Name</u>	<u>Sequence</u>	<u>Used for</u>
EOO-042 / pFA6a Fw	TCGTACGCTGCAGGTCGACGGATCCCC	amplification of marker cassette
EOO-043 / pFA6a Rv	ATCGATGAATTCGAGCTCGTTTAAAC	amplification of marker cassette
EOO-139 dh Fw	CTCTCATCTCGACTCGTTTG	ChIP, RT-PCR
EOO-140 dh Rv	GGCATTACGAAACATAGCG	ChIP, RT-PCR
EOO-482/ade6 Fw	GTAGTACGCAGTTTACGACGG	ChIP
EOO-483/ade6 Rv	GAGCACGCTGTTGAATTGAG	ChIP, Northern analysis
EOO-484/ura4 Fw	GAATGGTTTGAGAAGCATACC	ChIP
EOO-485/ura4 Rv	GAGTACGATATTGCTGTCCC	ChIP, Northern analysis
EOS-141/act1 Fw	TGCCGATCGTATGCAAAAAGG	ChIP, RT-PCR
EOS-142/act1 Rv	CCGCTCTCATCATACTCTTG	ChIP, RT-PCR
KKO-480/fbp1 Fw	GTCGAACGGATGCTGCAAAAC	ChIP
KKO-481/fbp1 Rv	GGTACCTACACTAACACCGG	ChIP
KKO-482/adh1 Fw	GGTGTCAAGTGGATGAACTC	ChIP
KKO-483/adh1 Rv	GCATTGGCAATGCAGTAGTG	ChIP
EOS-451/ SPCTRNAASN.05 Fw	AATATATCAAGCAAGAATGGGG	ChIP
EOS-450/ SPCTRNAASN.05 Rv	CGACCTCACGATTAACAGTCG	ChIP, siRNA analysis
EOS-513/ gene free region Fw	CAGTGGTAAGGGATTGTTGTAAGG	ChIP
EOS-514/ gene free region Rv	TGGCATAGAGGACGGAAGG	ChIP
EOS-529 cenH dh Fw	GCTAAGATCGATTGGTGACG	ChIP, RT-PCR
EOS-530 cenH dh Rv	AAGTTCACTGTTCTTATACACTGG	ChIP, RT-PCR
EOS-495/SPRRNA.48 Fw	AACAGCCTCTAGTGCAGATC	ChIP, RT-PCR
EOS-496 / SPRRNA.48 Rv	GAGCTTCCCTATCTCTTAGG	ChIP, RT-PCR
EOO-517/dh Fw	ACAACGCATCTACCTCAGCAGTCCTTGGG	Northern analysis
EOO-518/dh Rv	CCCAAGGACTGCTGAGGTAGATGCGTTGT	Northern analysis
EOO-519/dg Rv	CCATCCGCAGTTGGGAGTACATCATTCC	Northern analysis
EOO-520/dg Fw	GGAATGATGTACTCCCAACTGCGGATGG	Northern analysis
KKO-586/cen siRNA A	GCGACTAAACCGAAAGCCTC	siRNA analysis
KKO-587/cen siRNA B	TACCGTGATTAGCCTTACTCCGCATT	siRNA analysis
KKO-588/cen siRNA C	TACTTATTGATGGCGAAGCTAGA	siRNA analysis
KKO-589/cen siRNA D	TACCGCTTCTCCTTAATCCA	siRNA analysis
KKO-590/cen siRNA E	ACACCTACTCTTACTACTTGT	siRNA analysis
KKO-591/cen siRNA F	GACGATAAGCAGGAGTTGCGCA	siRNA analysis
KKO-592/cen siRNA G	AGTGTGGCGCTATATCTTGTA	siRNA analysis
KKO-593/cen siRNA H	TACTGTTCATTAGGATATGCTCA	siRNA analysis
KKO-594/cen siRNA I	GGGAAATGTATAAATAGGCA	siRNA analysis
KKO-595/cen siRNA J	TTTCCCAAGGACTGCTGAGGTAGA	siRNA analysis
KKO-596/cen siRNA K	TGGACACAGCATGGATATGGACACA	siRNA analysis
KKO-597/cen siRNA L	TGGCAGATATTGCAAGTTGTTTA	siRNA analysis
KKO-623/cen siRNA-1	CCTTAATTA AAAACGACCAATATG	siRNA analysis
KKO-624/cen siRNA-2	CTGCGGTTACCCCTTAACATC	siRNA analysis
KKO-625/cen siRNA-3	CAACTGCGGATGGAAAAAGT	siRNA analysis
KKO-626/cen siRNA-4	CTCTATATATCAGATATAAAGATGCG	siRNA analysis
KKO-627/cen siRNA-5	GTTTTGAAGTAGACATTCCGCACAA	siRNA analysis
KKO-628/cen siRNA-6	CTGAGCACAAAGAGACATGGTGTACTAGA	siRNA analysis
KKO-629/cen siRNA-7	GTACATTTTGCAGGACAACCAG	siRNA analysis
KKO-630/cen siRNA-8	CAACAACAGTCTTGGATTTATTTAG	siRNA analysis
EOS-529/ cenH dh Rv	GCTAAGATCGATTGGTGACG	ChIP
EOS-530/ cenH dh Fw	AAGTTCACTGTTCTTATACACTGG	ChIP
EOS-219/ adh1 promoter Fw	TCTCATTGGTCTTCCGCTCC	ChIP-qPCR time course analysis
EOS-220/ adh1 promoter Rv	AAGAAAAGCGAAGGCACCTG	ChIP-qPCR time course analysis

III. Results

III-i. Mediator is required for heterochromatic silencing at the pericentromeres.

III-i-a. Loss of Mediator causes defects in heterochromatin-dependent gene silencing

To investigate whether Mediator is involved in heterochromatin assembly, each gene encoding a non-essential subunit of mediator was disrupted in strain possessing marker genes in the pericentromeric heterochromatin (*otr1R::ade6⁺* and *imr1L::ura4⁺*) to monitor heterochromatic silencing (Figure 4A) [35]. Since the *otr1R::ade6⁺* and *imr1L::ura4⁺* genes are repressed by heterochromatin, the wild-type strain formed red colonies on a solid medium containing a limiting amount of adenine (Low Ade) and was resistant to 5-fluoroorotic acid (5-FOA), a counter-selective drug for *ura4⁺* expression. By contrast, heterochromatin mutants, such as *clr4Δ*, formed white or pink colonies on the Low Ade plate and showed sensitivity to 5-FOA (Figure 4B). Among the eight non-essential subunits of mediator tested (*med1/pmc2*, *med27/pmc3*, *med18/pmc6*, *med20*, *med19/rox3*, *med12/srb8*, *med13/srb9* and *cdk8/srb10*), only disruption of *med18* (also called as *pmc6*) and *med20* resulted in the formation of pink colonies and increased sensitivity to 5-FOA (Figure 4B), which is coupled with growth on plates lacking uracil or adenine (Figure 5A). Closer examination revealed that both *med18Δ med20Δ* cells formed a mixture of white and pink colonies on Low Ade plates. In addition, point mutants of *med8* (*med8-K9*) and *med31* (*med31-H1*), which were isolated by the screening of heterochromatic mutants (Figure 5B; Kato et al. submitted), also formed a mixture of pink and white colonies (Figure 4C, Figure 4C).

III-i-b. Loss of Mediator shows variegated phenotype

The variegation in the color of colonies by the mutation of Mediator subunits suggested that silencing of the *otr1R::ade6⁺* gene was variegated in the mutant cells and that distinct levels of *otr1R::ade6⁺* silencing were epigenetically inherited. To test the stability of the pink and white phenotype, pink and white colonies of each mutant were selected, cultured in YES media overnight and re-spotted onto Low Ade

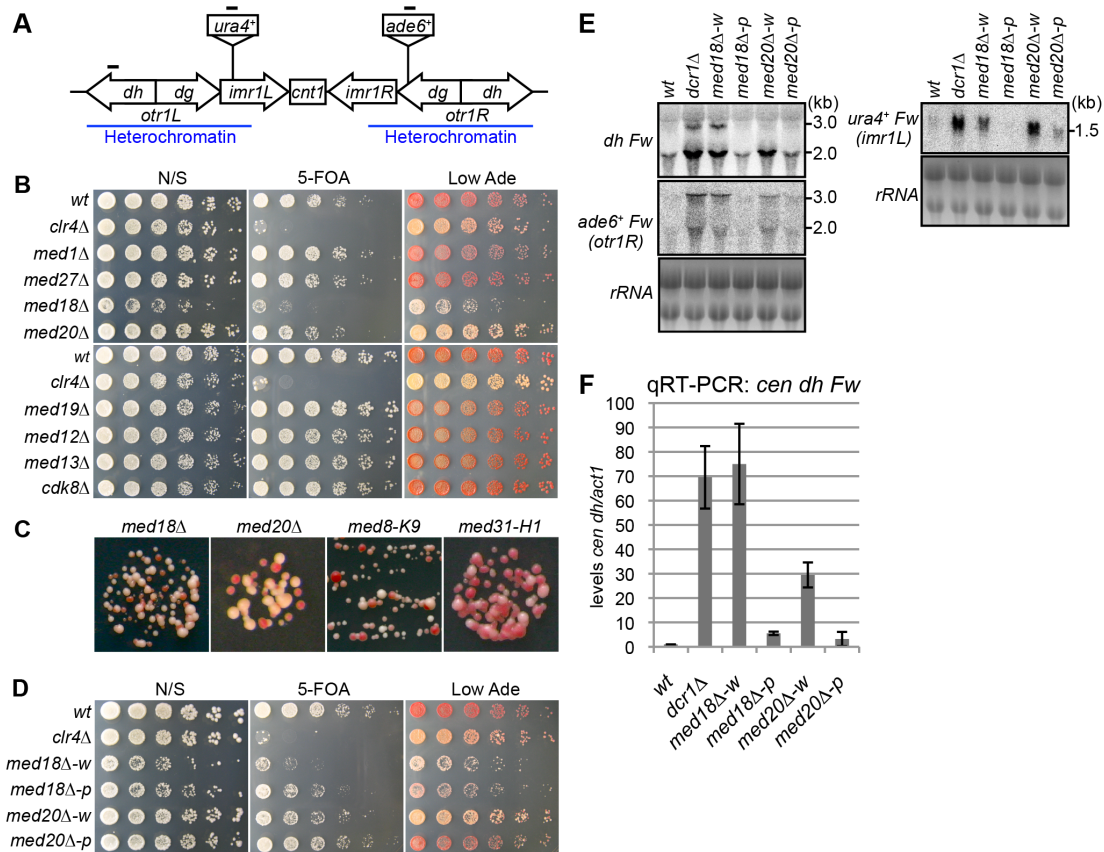


Figure 4. Mediator is required for heterochromatic silencing at the pericentromere.

(A) Schematic of fission yeast centromere 1. Locations of *ura4* and *ade6* reporter genes inserted within the pericentromeric region are shown (*imr1L::ura4⁺* and *otr1R::ade6*). Black bars indicate the location of primers or probes used for ChIP, RT-PCR and northern analysis. (B) Silencing assay at the pericentromere. Shown are the results of serial dilutions of the indicated strains spotted onto non-selective media (N/S), medium with 5-fluoroorotic acid (5-FOA), and medium with a limiting amount of adenine (Low Ade) to assay *ura4⁺* and *ade6⁺* expression. (C) Spots on Low Ade medium using Mediator mutants (*med18Δ*, *med20Δ*, *med8-K9* and *med31-H1*), which are defective in heterochromatic silencing at the pericentromere. (D) Silencing assay at the pericentromere. Shown are the results of serial dilutions of the indicated strains spotted onto N/S, 5-FOA and Low Ade media to assay *ura4⁺* and *ade6⁺* expression. *w* indicates white epiclones (*med18Δ-w* and *med20Δ-w*), and *p* indicates pink epiclones (*med18Δ-p* and *med20Δ-p*). (E) Northern Analysis of *dh*, *otr1R::ade6* and *imr1L::ura4* forward strand transcripts in wild-type (*wt*) and mutant cells using oligonucleotide probes. rRNA was used as a loading control. (F) Quantitative RT-PCR analysis of *cen dh* forward transcript levels relative to a control *act1⁺*, normalized to the wild type in the indicated strains. Error bars show the standard error of the mean (n = 3).

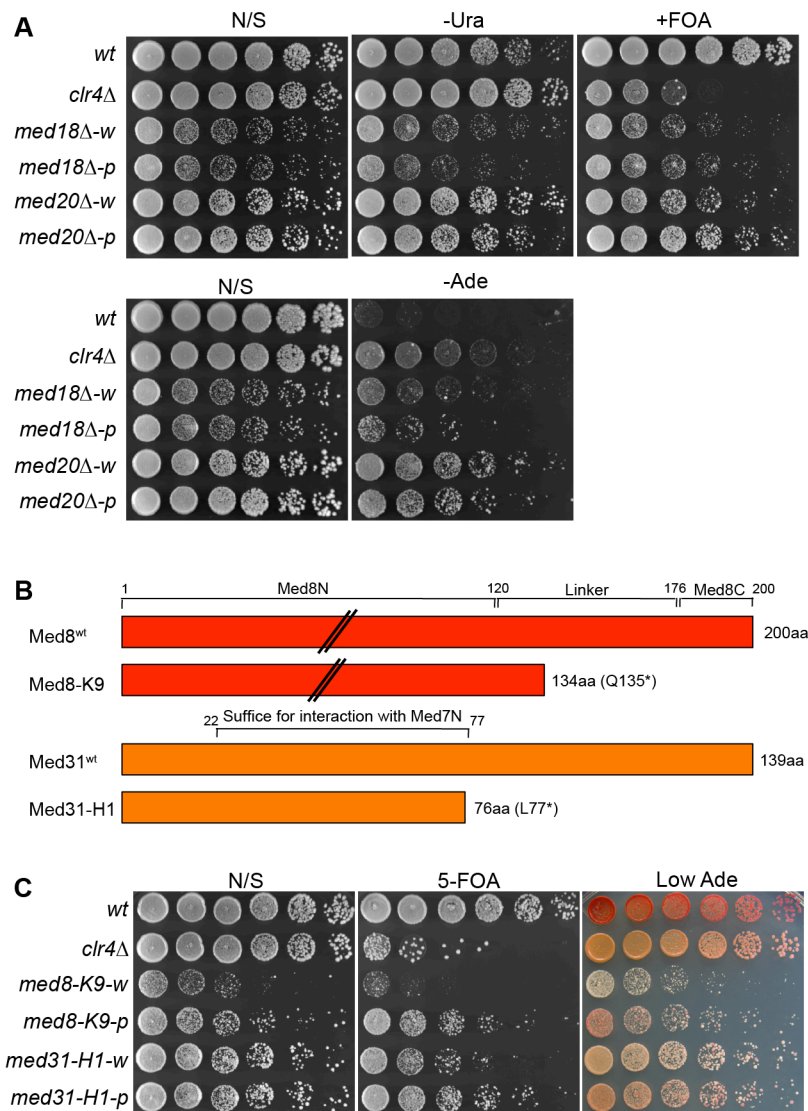


Figure 5. Mediator is required for heterochromatin silencing at the pericentromere.

(A) Silencing assay at the pericentromere. Shown are the results of serial dilutions of the indicated strains spotted onto non-selective media (N/S), medium without adenine (-Ura), medium with 5-fluoroorotic acid (5-FOA), and medium without adenine (-Ade) to assay *ura4⁺* and *ade6⁺*. Note that PMGS (EMMS-NH₄Cl (nitrogen), +L-glutamic acid, monosodium, as nitrogen) plates were used as N/S plates. (B) Schematic of Med8-K9 and Med31-H1 proteins. *med8-K9* contains a point mutation (C540T) causing C-terminal truncation of the Med8 protein (Q135*) (top). The C-terminal residues 176–200 of Med8 (Med8C) are the predicted interface for interaction with Med18 [24, 36]. *med31-H1* contains a point mutation (T230A) causing C-terminal truncation of the Med31 protein (L77*) (bottom). Residues 22–77 of Med31 are the predicted interface for interaction with Med7, a core Mediator subunit belonged to the middle domain. (C) Silencing assay at the pericentromere. Shown are the results of serial dilutions of the indicated strains spotted onto non-selective media (N/S), medium with 5-fluoroorotic acid (5-FOA), and medium with a limiting amount of adenine (Low Ade) to assay for the presence of *imr1L::ura4⁺* and *otr1R::ade6⁺*.

and 5-FOA plates. Re-spotting of the cells from white colonies (*med18Δ-w*, *med20Δ-w* and *med8-K9-w*) and pink colonies (*med18Δ-p*, *med20Δ-p* and *med8-K9-p*) produced predominantly white colonies and pink colonies, respectively (Figure 4D, Figure 5B). This indicated that the white and pink phenotypes were epigenetically inherited through generation but exchangeable, which is confirmed by the measurements of the conversion rates between white and pink epiclones (Figure 6). The conversion rates are different in each mutants, but in all mutants, conversion rates from pink to white is higher than those of white to pink, showing that white-epiclones, in which heterochromatin is compromised, are more stable. Hereafter, we designate the epigenetic clones derived from white colonies and red colonies as white and pink “epiclones”, respectively. *med18Δ-w* and *med20Δ-w* showed greater sensitivity to 5-FOA than *med18Δ-p* and *med20Δ-p* (Figure 4D), indicating that the silencing defect at *otr::ade6⁺* couples with that at *imr::ura4⁺* and that silencing at *imr::ura4⁺* was also compromised more severely in the white epiclones. This suggested that the white phenotype reflected silencing defects of the entire pericentromeric heterochromatin. It should be noted that it was difficult to separate the white epiclones from the pink epiclones of *med31-H1* cells (*med31-H1-w* and *med31-H1-p* in Figure 5B) because of frequent variegation between the two (Figure 6).

III-i-c. Loss of Mediator causes the accumulation of transcripts from pericentromeric region.

The loss of heterochromatic gene silencing was confirmed in Mediator mutants by measuring the accumulation of transcripts from the pericentromeric repeats (*dg* and *dh*) and inserted marker genes. Strand-specific northern analysis showed a large increase in those transcripts in both *med18Δ-* and *med20Δ-w* cells (Figure 4E and Figure 7), which was consistent with the observed silencing defects (Fig 4D), while only marginal accumulation was observed in *med18Δ-p* and *med20Δ-p* cells. Both point mutants of the other Mediator subunits (*med8-K9* and *med31-H1*) also showed accumulation of the transcripts (Figure 7). Accumulation of heterochromatic transcripts from *dh* repeats was also demonstrated by strand-specific RT-PCR (Figure 4F). These results showed that the Mediator subunits Med8, Med18, Med20 and Med31 were involved in silencing pericentromeric heterochromatin. Med18 and Med20 form a heterodimer that associates with head domain core complex through Med8 [24], and the connection between the Med18/Med20

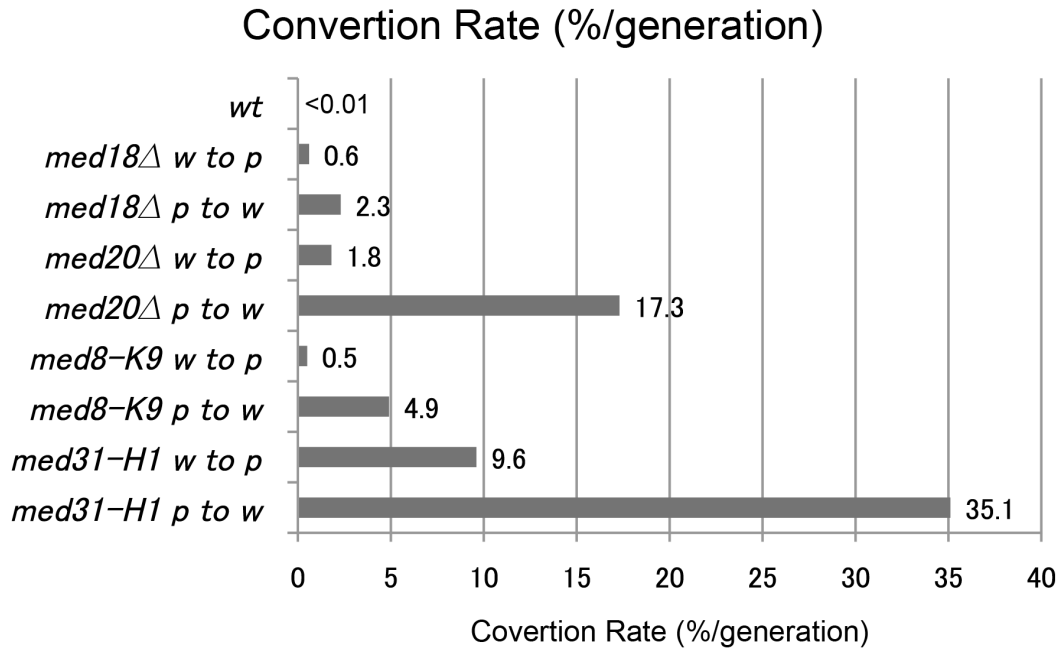


Figure 6. Conversion rates of white/pink epiclones.

Stability assay of variegation phenotypes. Conversion rates (percentage of cells that convert epiclone's color per generation) were measured using indicated strains. *w* indicate the white epiclones and *p* indicate the pink epiclones. Cells were grown for several generations. The rates were measured as described in supplemental experimental procedures.

heterodimer and head domain appears to be lost in the *med8-K9* mutant (Figure 5A). In addition, Med31, a component of the middle domain, is located close to the head domain. Thus, because these findings indicate that Mediator functions in pericentromeric heterochromatin via the head domain, Med18 and Med20 were selected for closer examination.

III-i-d. Conclusion

Loss of Mediator caused disruption of heterochromatin-dependent gene silencing and the accumulation of transcripts at pericentromere. In addition, Mediator mutants showed variegated phenotype that silencing of the *otr1R::ade6⁺* gene was variegated. Thus, Mediator functions in heterochromatic silencing via the head domain.

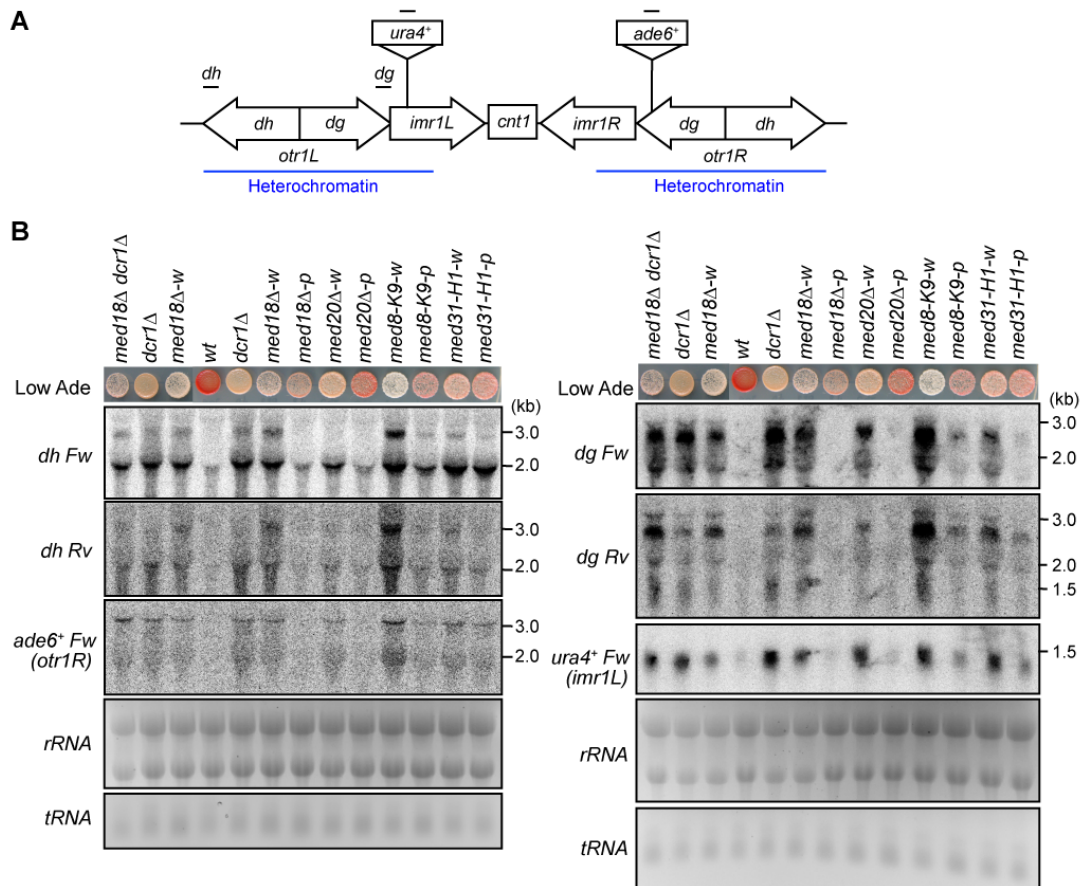


Figure 7. Mediator mutants cause accumulation of centromeric RNA

(A) Schematic of fission yeast centromere 1. Locations of the *ura4⁺* and *ade6⁺* reporters inserted within the pericentromeric region are shown (*imr1L::ura4⁺* and *otr1R::ade6⁺*). Black bars indicate the location of probes used for northern analysis. (B) Northern analysis of pericentromeric transcripts in wild-type and mutant cells. Analysis was performed using oligonucleotide probes against *dh* and *dg* forward (Fw) and reverse (Rv) strands, *imr1L::ura4⁺* and *otr1R::ade6⁺* forward strand transcripts. rRNA and tRNA were used as loading controls.

III-ii. Mediator localizes with RNAPII at the pericentromeric repeats.

III-ii-a. Mediator localizes pericentromeric heterochromatin with RNAPII in cell cycle dependent manner.

Both RNAi- and Rrp6-dependent heterochromatin formation, which occur in parallel at the pericentromere, appear to be coupled to the transcription of ncRNA at the pericentromeric repeats [10, 18]. Hence, it appeared that Mediator contributed to pericentromeric heterochromatin formation directly through the transcription of ncRNA and/or processing of ncRNA. If this assumption was true, Mediator should localize to the transcribed region in heterochromatic repeats. To test this possibility, the localization of Med20-5Flag and RNAPII to the transcribed regions of *dh* repeats was examined by ChIP assay. Since heterochromatic ncRNA is mainly transcribed during G1/S-phase [11], cell cycle was synchronized using the *cdc25* temperature-sensitive mutant strain. The results show that RNAPII accumulated during G1 to early S-phase, followed by the accumulation of transcripts (Figure 8A, D). Med20-5Flag showed a similar oscillating pattern, but the peak disappeared slightly earlier than the Pol2 peak (Figure 8B). This is consistent with the speculation that Mediator is involved in heterochromatic ncRNA transcription.

III-ii-b. Conclusion

Mediator localizes pericentromeric heterochromatin with RNAPII during G1-S phase. This result suggests that Mediator is involved in heterochromatic ncRNA transcription.

III-iii. Loss of Med18 or Med20 causes defects in heterochromatin structure at the pericentromeres.

III-iii-a. Loss of Med18/20 causes defects in heterochromatin structure at the pericentromeres.

To gain further insight into the roles of Mediator during heterochromatin organization, the occupancy of H3K9me2, Swi6 and RNAPII at the centromeric heterochromatin was assessed by chromatin immunoprecipitation (ChIP) analysis. At

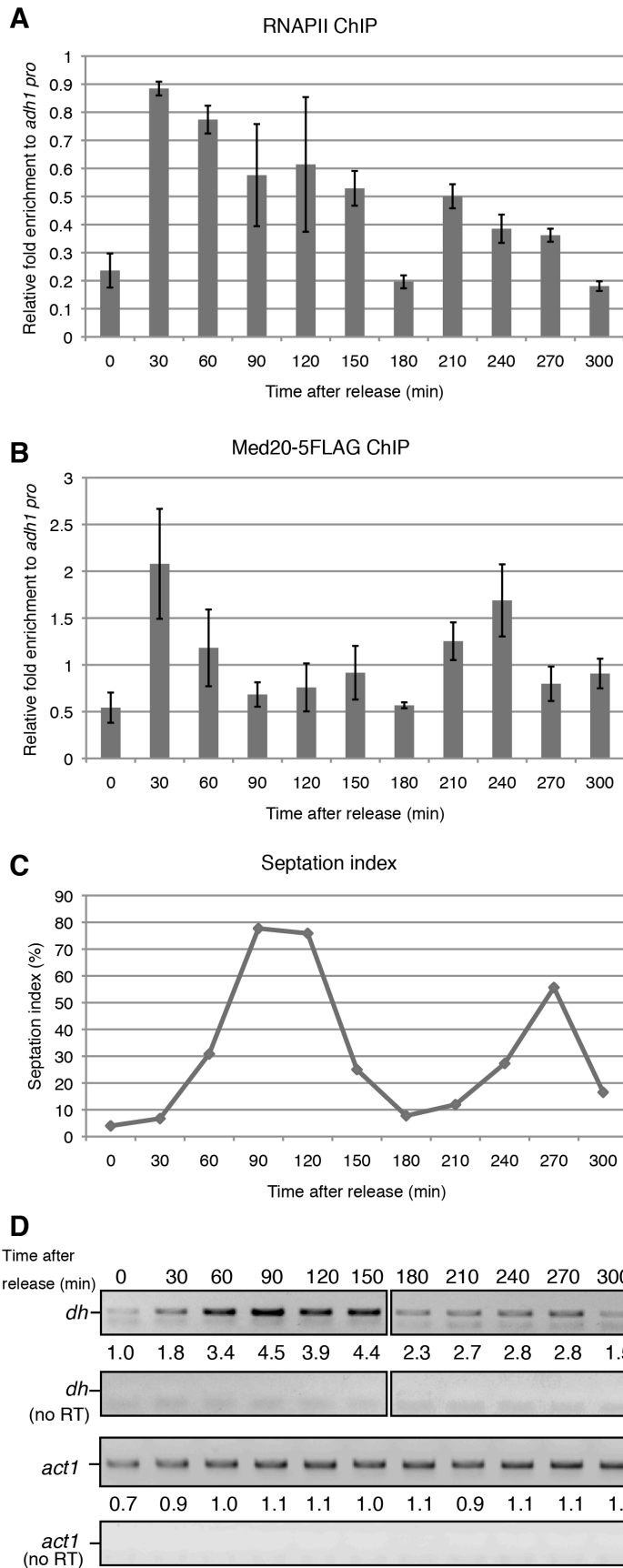


Figure 8. Med20 localizes pericentromeric heterochromatin with RNAPII in a cell cycle-dependent manner
 (A, B) ChIP-qPCR analyses for RNAPII and Med20-5FLAG were performed every 30 minutes after release from G2/M block by *cdc25-22* mutation (see Supplemental Experimental Procedures). Enrichment at *dh* repeats relative to the *adh1* promoter region (*adh1 pro*) is shown. Error bars show the standard error of the mean (n = 3). (C) Septation index (percentage of cells with division septum) was measured to monitor cell cycle progression after release. The peak of septation (90 to 120 min) indicates S phase. (D) RT-PCR of *dh* transcripts was performed as described in A and B. Transcripts derived from constitutively expressed *act1* served as controls. “No RT” indicates that no reverse transcriptase was added in the reaction. Numbers under the panels of *dh* and *act1* indicate the increase in transcript relative to the values at 0 min (*dh*) and 60 min (*act1*), respectively.

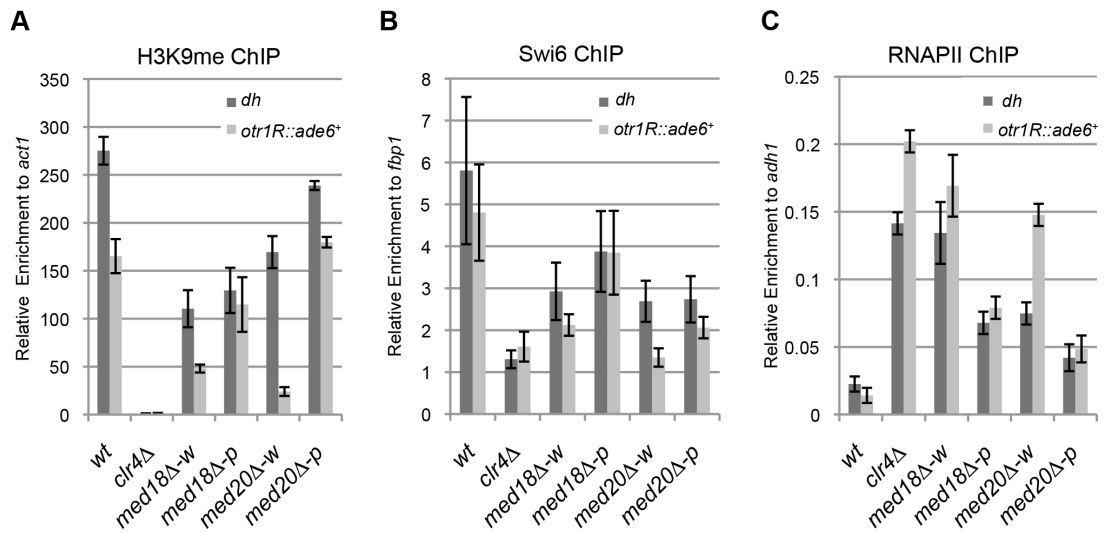


Figure 9 Loss of Med18/20 causes defects in heterochromatin structure at the pericentromere.

ChIP analysis of H3K9me2 (A), Swi6 (B) and RNAPII (C) at *dh* repeats or *otr1R::ade6⁺* relative to *act1*, *fbp1* or *adh1*, respectively. Error bars show the standard error of the mean (n = 3).

the inserted marker gene (*otr1R::ade6⁺*), the levels of histone H3K9me2 and Swi6 were decreased and RNAPII occupancy was increased in the white epiclones of *med18Δ* and *med20Δ* cells (Figure 9A-C). This indicated that heterochromatin structure at the marker gene was disrupted in the white epiclones. By contrast, in the pink epiclones of *med18Δ* and *med20Δ* cells, the decrease in H3K9me/Swi6 and increase in RNAPII were less prominent than those in white epiclones. This reflected the difference in silencing defects in each epiclone (Figure 4D). At the heterochromatic repeats, *dh*, H3K9me/Swi6 and RNAPII were also decreased and increased in the Mediator mutants, respectively, but the differences between the white and pink epiclones were less prominent than at *otr1R::ade6⁺*.

III-iii-b. Conclusion

These results showed that the accumulation of transcripts from heterochromatic repeats and marker genes is, at least in part, due to an increase in transcription induced by the disruption of heterochromatin structure. These results also confirm that Mediator is required for heterochromatin formation at the pericentromere.

III-iv. Med18 is required for Rrp6-dependent H3K9 methylation at the pericentromere.

III-iv-a. Med18 functions in a pathway distinct from the RNAi-dependent pathway.

There are two distinct pathways for heterochromatin formation at the pericentromeric repeats: RNAi-dependent and Rrp6-dependent pathways. In RNAi mutants such as *dcr1Δ*, H3K9me is diminished at the inserted marker genes but substantially retained at the pericentromeric repeats, while disruption of *rrp6* did not affect H3K9 me at the marker genes [18]. The distribution of H3K9me in the white epiclones of the Mediator mutants resembled that observed in *dcr1Δ* cells; the level of H3K9me at the marker genes was lower than that at heterochromatic repeats. Thus, We speculated that Mediator is involved in the RNAi-dependent pathway. To confirm this, a *med18Δdcr1Δ* double mutant was established and used to examine

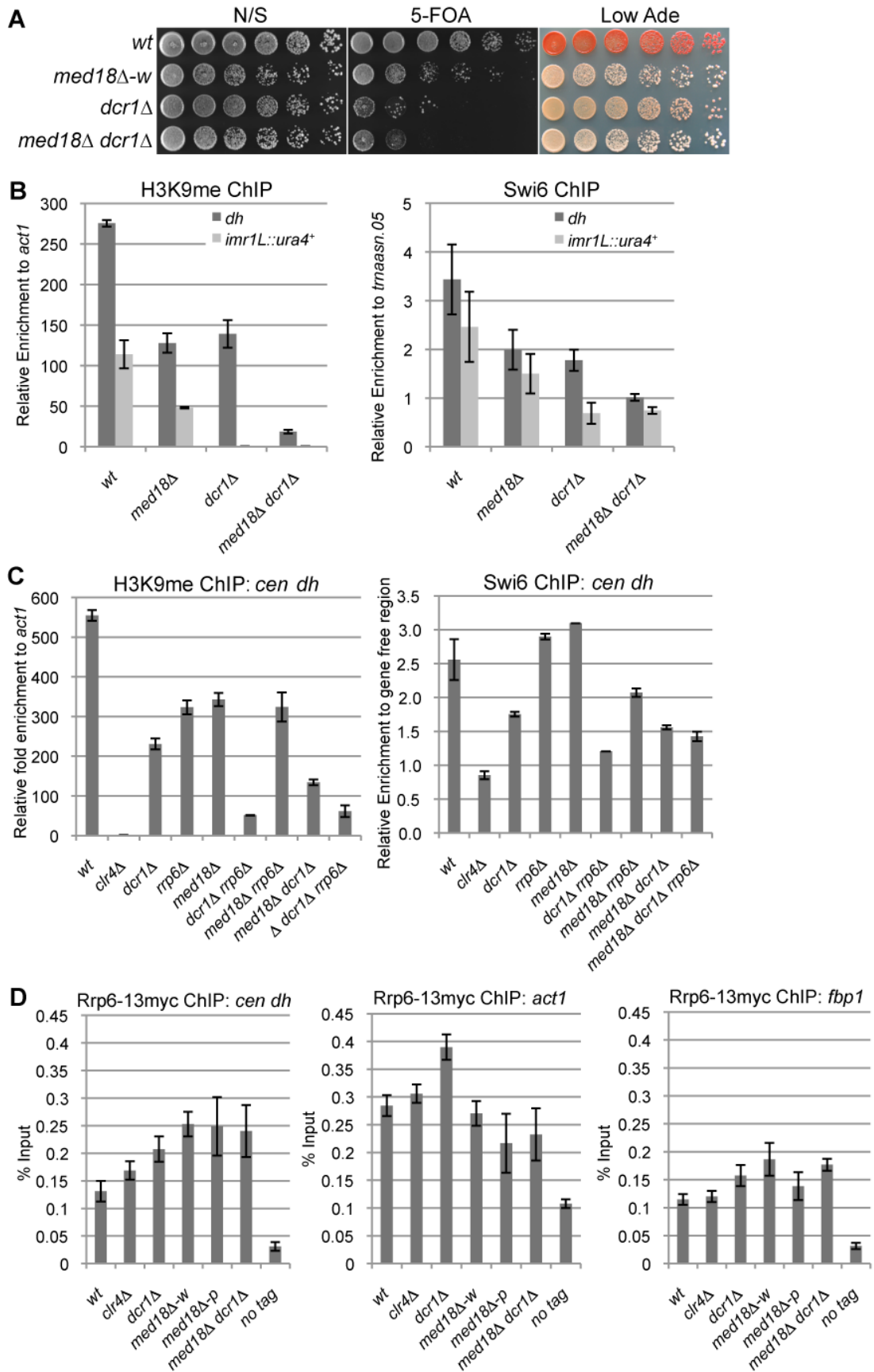


Figure 10. Med18/Mediator is required for Rrp6/Exosome-dependent H3K9 methylation at the pericentromere.

(A) Silencing assay at the pericentromere. Shown are the results of serial dilutions of the indicated strains spotted onto N/S, 5-FOA and Low Ade media to assay *ura4⁺* and *ade6* expression. (B) ChIP analysis of H3K9me2 (left panel) and Swi6 (right panel) at *dh* repeats or *imr1L::ura4⁺* relative to *act1* or *trnaasn.05*, respectively. Error bars show the standard error of the mean (n = 3). (C) ChIP analysis of H3K9me2 (left panel) and Swi6 (right panel) at the *dh* repeats relative to *act1* or a gene-free region, respectively. Error bars show the standard error of the mean (n = 3). (D) ChIP analysis of Rrp6-13myc at *dh* repeats, *act1* and *fbp1*. Enrichment relative to input WCE in the indicated strains are shown. Error bars represent the standard error of the mean (n = 3).

heterochromatin silencing and the amount of H3K9me and Swi6 at *dh* repeats and *otr1R::ade6⁺* (Figure 10A, B). Note that since $\Delta med18\Delta dcr1$ cells did not exhibit the variegated phenotype observed in the *med18* Δ single mutant (Figure 10), white and pink epiclones of *med18* Δ cells were not separated in this experiment as shown in Figure 1B and C. If Mediator functions in the RNAi-dependent pathway, the *med18* $\Delta dcr1$ Δ double mutants would retain amounts of H3K9me and Swi6 similar to that of each single mutant. However, in the double mutant, the retained H3K9me/Swi6 at the *dh* repeats was significantly decreased compared to each single mutant (Figure 10B), suggesting that, contrary to our speculation, Med18 functions in a pathway distinct from the RNAi-dependent pathway.

III-iv-b. Med18 is required for Rrp6-dependent H3K9 methylation at the pericentromere.

Because the results in Figure 9B were reminiscent of the results reported by Reyes-Trucu et al., in which the amount of H3K9me retained at the centromeric repeats in *ago1* Δ cells was significantly decreased by further disruption of *rrp6* [18], we speculated that Mediator functioned in an Rrp6-dependent heterochromatin formation pathway. To confirm this, single, double and triple mutants of *dcr1*, *med18* and *rrp6* were established and used to measure the amount of H3K9me at the *dh* repeats (Figure 9C, left panel). Each single mutant, as well as the *med18* $\Delta rrp6$ Δ double mutants, retained similar amounts of H3K9me. By contrast, combination of *dcr1* Δ with *rrp6* Δ caused a substantial decrease in H3K9me, which was consistent with the previous proposal that both RNAi- and Rrp6-dependent pathways contribute to heterochromatin formation at the pericentromeres [18]. Similarly, the combination of *dcr1* Δ with *med18* Δ also caused a significant decrease in H3K9me, while *med18* $\Delta rrp6$ Δ cells maintained a level of H3K9me comparable to each single disruptant. The H3K9me retained in *med18* $\Delta rrp6$ Δ cells was also decreased by the introduction of *dcr1* Δ . The amount of Swi6 in each mutant reflects the amount of H3K9me (Figure 10C, left panel). These results clearly indicate that Med18 functions in the same heterochromatin formation pathway as Rrp6 at the *dh* repeats. Therefore, H3K9me in *dcr1* Δ cells was retained by the Rrp6/Med18-dependent pathway, while H3K9me in *med18* Δ and *rrp6* Δ cells was maintained by the RNAi-dependent pathway.

III-iv-c. Mediator might functions in a step after association of Rrp6 on chromatin for heterochromatin formation.

Details of the Rrp6-dependent pathway are not clear yet; even the localization of Rrp6 at heterochromatin has not been examined. We, thereby, analyzed the localization of Rrp6 tagged with myc epitope at heterochromatin (*dh*) as well as euchromatin (*act1* and *fbp1*) (Figure. 10D). Rrp6-myc was enriched at both *dh* and euchromatic genes to the same extent compared with no-tag control. Depletion of *clr4* did not affect the localization of Rrp6-myc, while deletion of *dcr1* caused a slight increase at all loci. The enrichment of Rrp6 marginally changed in *med18Δ-w* and *med18Δ-p* epiclones, and also in the *med18Δdcr1Δ* double mutant. This suggests that Mediator functions in a step after association of Rrp6 on chromatin for heterochromatin formation.

III-iv-d. Conclusion

These results indicate that Med18 functions in the same heterochromatin formation pathway as Rrp6 at the *dh* repeats. The ChIP analysis also suggests that Mediator functions in a step after association of Rrp6 on chromatin for heterochromatin formation.

III-v. Mediator is required for the generation of siRNA from pericentromeric ncRNA.

III-v-a. Med18/Mediator is also involved in the RNAi-dependent heterochromatin pathway.

Both *dcr1Δ* and *rrp6Δ* cells retained similar levels of H3K9me at centromeric repeats (Figure 10B). By contrast, deletion of *rrp6* does not affect H3K9me at the marker genes inserted in centromeric repeats [18], whereas deletion of *dcr1* caused the loss of H3K9me on the marker genes (Figure 10B), indicating that the spreading of H3K9me into the inserted marker genes occurs via an RNAi-dependent mechanism [14, 15]. While H3K9me at *otr1R::ade6⁺* was severely decreased in the white epiclones of *med18Δ* and *med20Δ*, it was substantially retained in the pink epiclones (Figure 8A), indicating that the spreading of H3K9me was variegated in the Mediator mutants. As shown in Figure 9A, *med18Δdcr1Δ* cells did not exhibit a variegated

phenotype. These data confirm that the loss of Med18/Mediator results in the variegation of RNAi-dependent heterochromatin spreading. In other words, Med18/Mediator is also involved in the RNAi-dependent heterochromatin pathway.

III-v-b. Mediator is required for siRNA formation at the pericentromeric repeats.

To examine the involvement of Mediator in RNAi, siRNA derived from *dg* and *dh* repeats was analyzed in the Mediator mutants. siRNAs corresponding to the pericentromeric repeats were not detected in *dcr1Δ* cells (Figure 11A). In the white epiclones of the Mediator mutants, a marginal amount of siRNA from the *dg* and *dh* repeats was detected (Figure 11A and Figure 12A, B). The marginal amount of siRNA was diminished by introduction of *dcr1Δ* (Figure 12B), showing that the siRNA observed in *med18Δ* cells are produced through RNAi pathway. In the pink epiclones, reduced but significant amounts of siRNAs (approximately 10–50% of that of wild-type cells) were detectable. Note that the amount was varied because of the state of variegation. Since the structure of heterochromatin (H3K9me and Swi6) at the repeats was substantially maintained in both white epiclones (Figure 10A, B) and the maintenance was dependent upon RNAi-pathway as shown above (Figure 9C), the small amount of siRNA synthesized in the white epiclones appears to be sufficient to maintain heterochromatin structure at the repeats. A similar reduction of siRNA was observed in the white and pink epiclones of *med8-K9* cells and *med31-H1* cells (Figure 12). Note that when siRNA derived from *dg* and *dh* repeats was analyzed separately, each siRNA was found to be reduced in *med18Δ* cells (Figure 12). These data indicate that Mediator is required for siRNA generation at pericentromeric heterochromatin and the defect of the Mediator head domain causes variegation of the spreading of H3K9me into the marker genes.

III-v-c. Conclusion

These data suggest that Mediator is also involved in the RNAi-dependent heterochromatin pathway, especially in siRNA synthesis.

III-vi. Mediator promotes efficient siRNA formation from RITS-bound ncRNA.

III-vi-a. Mediator is not required for the step of the association of the RITS complex and RDRC to heterochromatin.

Since RNAi machinery localizes on heterochromatin for processing of ncRNA into siRNA [3, 6, 12, 37], the requirement of Med18 for the recruitment of RNAi factors to heterochromatin was investigated. Binding of the components of the RITS complex (3Flag-Ago1 and Chp1-5myc) and of RDRC (Rdp1-5Flag) to pericentromeric repeats was examined by ChIP assay (Figure 11B-D). As reported, 3Flag-Ago1 bound to *dh* repeats in a heterochromatin- and/or RNAi-dependent manner [3, 12, 37], as evidenced by the finding that the binding of Ago1 was reduced to a level comparable to that of the no-Flag-tag control in *clr4* Δ and *dcr1* Δ cells. By contrast, a substantial amount of 3Flag-Ago1 was retained in *med18* Δ cells that formed a mixture of pink and white epiclones (Figure 11B left panel). Binding of Chp1-13myc to *dh* repeats was abolished by deletion of *clr4*, while reduced but significant Chp1-13myc localization was observed at the *dh* repeats in *dcr1* Δ cells, representing the binding of the chromo-domain of Chp1 to H3K9me that was retained at the pericentromeric repeats in these cells (Figure 11C, right panel). By contrast, the binding of Chp1-13myc was not affected by the deletion of *med18*. Even in white epiclones, in which H3K9me is reduced to the same level as in *dcr1* Δ cells (Figure 11C, right panel), Chp1-13myc binds to *dh* repeats at the same level as in wild-type cells (Figure 11C, left panel). Association of Rdp1-5Flag in each mutant was similar to that of 3Flag-Ago1 in that it was almost abolished in *clr4* Δ and *dcr1* Δ cells, but significantly retained in both *med18* Δ -*w* and *med18* Δ -*p* cells (Figure 11D, left panel). All together, the RITS complex and RDRC associated with heterochromatin even in *med18* Δ -*w* cells, probably because the small amount of siRNA synthesized in *med18* Δ cells was sufficient for the association of RITS with heterochromatin. These data, together with the data on the accumulation of ncRNA and reduction of siRNA in Mediator mutants, indicate that Mediator is not required for the association of the RITS complex and RDRC to heterochromatin but is required for efficient siRNA production by heterochromatin-bound RNAi machinery.

III-vi-b. Mediator plays a role in the step following the binding of the RITS complex to target RNA.

It has been previously reported that the tethering of RITS to *ura4* RNA induces RNAi- and heterochromatin-dependent gene silencing of the *ura4* gene,

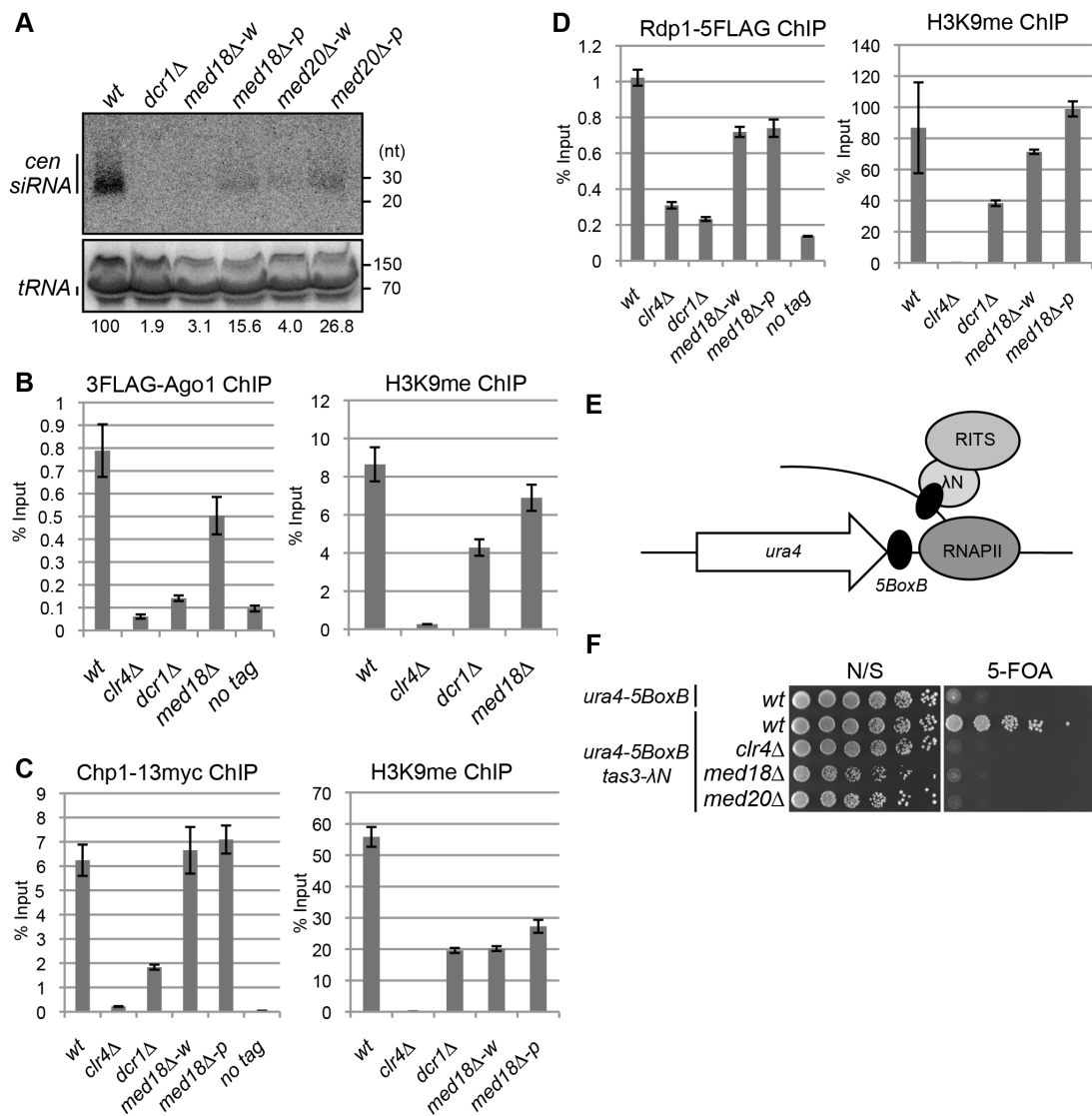


Figure 11. Mediator is required for siRNA formation at the pericentromeric repeats.

(A) Northern analysis of siRNA isolated from the indicated strains using oligonucleotide probes specific for *dg* and *dh* centromeric repeats. tRNA was used as a loading control. (B) ChIP analysis of 3× Flag-Ago1 and H3K9Me2 at *dh* repeats and *otr1R::ura4⁺* relative to input WCE in the indicated strains. Error bars show the standard error of the mean (n = 3). (C) ChIP analysis of Chp1-13x myc and H3K9me2 at *dh* repeats *imr1L::ura4⁺* and *otr1R::ade6⁺* relative to input WCE in the indicated strains. Error bars show the standard error of the mean (n = 3). (D) ChIP analysis of Rdp1- 5× flag and H3K9me2 at *dh* repeats *imr1L::ura4⁺* and *otr1R::ade6⁺* relative to input WCE in the indicated strains. Error bars show the standard error of the mean (n = 3). (E) Schematic representation of artificial heterochromatin formation by RNA-induced transcriptional silencing (RITS) tethering to the *ura4* mRNA. In this system, RITS was tethered artificially to *ura4* RNA via binding of the loss of *ura4-5BoxB* silencing (Figure 10F), similar to the effect of *clr4* disruption. λN protein fused to Tas3 (a subunit of RITS) to its recognition sequence, BoxB, five copies of which are

inserted into the 3' UTR of the *ura4* mRNA. This induced siRNA generation and subsequent heterochromatin formation at the *ura4* locus in an RNAi-dependent manner. (F) Gene silencing of *ura4* via tethering of RITS. Serial dilution of strains harboring the RITS-tethering system (*ura4-5boxB, tas3λN*) or *ura4-5boxB* alone were spotted onto N/S, 5-FOA and Low Ade media for silencing of the *ura4* gene. A strain harboring *clr4Δ* was also included as a control.

indicating that binding of the RITS complex to ncRNA is a key step in the RNAi-directed formation of heterochromatin by inducing H3K9 methylation and conversion of ncRNA to siRNA [38]. Tethering of RITS is achieved by the fusion of Tas3, a subunit of the RITS complex, to the λ N protein, which binds to the 5BoxB sequence inserted at the 3' UTR region of *ura4* RNA (Figure 11E). To determine whether Med18 or Med20 is required for Tas3- λ N-induced silencing of the *ura4-5boxB* gene, the effect of the deletion of these subunits on silencing induced by artificial tethering of the RITS complex was examined. Disruption of *med18* or *med20* resulted in the

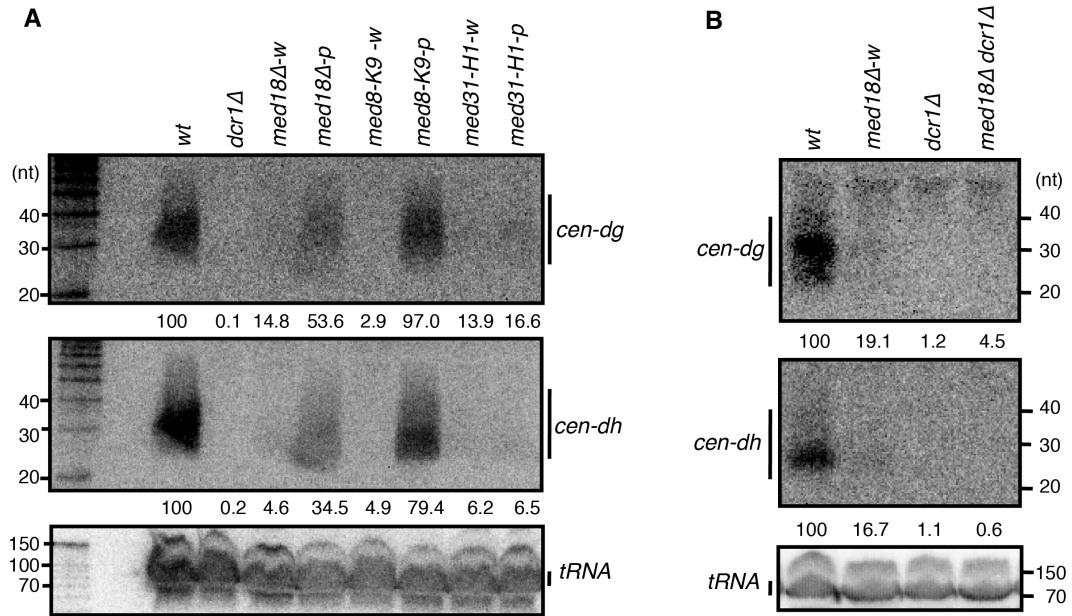


Figure 12. Northern analysis of siRNA in the Mediator mutants *med8-K9* and *med31-H1*. Analyses were performed with RNA isolated from the indicated strains using oligonucleotide probes specific for *dg/dh* centromeric repeats. tRNA was used as a loading control.

loss of *ura4-5BoxB* silencing (Figure 11F), similar to the effect of *clr4* disruption. This result showed that Med18 and Med20 are required for Tas3- λ N-induced silencing of the *ura4-5BoxB* locus and that Mediator plays a role in the step following the binding of the RITS complex to target RNA.

III-vi-c. Conclusion

These results indicate that Mediator is not required for the association of the RITS complex and RDRC to heterochromatin but plays a role in the step following the binding of the RITS complex to target RNA. The role of Mediator is required for efficient siRNA production by heterochromatin-bound RNAi machinery.

III-vii. Mediator is required for efficient transcription in heterochromatin.

III-vii-a. Mutation of Mediator would not be expected to affect mating locus heterochromatin.

Since Mediator regulates general transcription in euchromatin, it is possible that it also regulates the transcription of heterochromatic non-coding RNA. Indeed, recent reports suggest a negative role of Mediator head domain subunits (Med18 and Med20) in heterochromatic transcription, based on the observation of an increase in the transcription of pericentromeric ncRNA in Mediator mutants [39, 40]. However, it is difficult to state conclusively whether the observed increase is due to the direct effects of the absence of Mediator because it is also possible that the deletion of Mediator subunits causes disruption of the heterochromatin, which secondarily induces an increase in transcription. To avoid this dilemma, heterochromatin at the mating locus was selected for examination (Figure 13A) because the RNAi-dependent pathway is dispensable for the maintenance of heterochromatin here due to the existence of another pathway mediated by the DNA-binding proteins Atf1/Pcr1 [41]. Thus, mutation of Mediator would not be expected to affect mating locus heterochromatin, making it possible to directly measure the effect of the mutation on transcription activity in heterochromatin.

First, a ChIP assay was performed for H3K9me and Swi6 to examine heterochromatin structure at the mating-type locus in various mutants using *cenH* specific primers (Figure 13B). As expected, high levels of H3K9me2 and Swi6 were

maintained at the *cenH* sequence at the mating locus and the inserted *ura4⁺* gene (*kint2::ura4⁺*) in *dcr1Δ* and *dcr1Δmed18Δ* mutants. In *med18Δ* cells, the level of H3K9me was decreased to half of that of wild-type cells for an unknown reason, but Swi6, which is essential for transcriptional gene silencing in heterochromatin, was maintained, consistent with silencing (Figure 13B). Hence, the Atf1/Pcr1-dependent pathway retains heterochromatin structure and silencing without Med18 function.

Next, the effect of deletion of *dcr1* and *med18* on the silencing of *kint2::ura4⁺* was examined (Figure 13C). While the wild-type strain was able to grow on a 5-FOA-containing plate but not on a uracil-lacking (-Ura) plate, the *clr4Δ* strain was hypersensitive to 5-FOA but grew well on an -Ura plate (Figure 13C), showing that *kint2::ura4⁺* was silenced and expressed, respectively, in each strain. By contrast, *dcr1Δ* cells, like the *clr4Δ* cells, hardly grew on 5-FOA containing media, while some cells were able to grow on an -Ura plate, suggesting that silencing is only weakly compromised in *dcr1Δ* cells. However, *med18Δ* cells showed a phenotype similar to that of wild-type cells, showing no silencing defect at the mating locus. Introduction of *med18Δ* to *dcr1Δ* cells suppressed the silencing defect detected on the -Ura plate. RT-PCR analysis of transcripts from *cenH* and *kint2::ura4⁺* was consistent with the silencing assay; more than 100-fold, approximately 40-fold, and approximately 10-fold accumulation of transcripts from *cenH* and *kint2::ura4* were observed in *clr4Δ*, *dcr1Δ* and *med18Δ* cells, respectively (Figure 13D). In addition, introduction of *med18Δ* into *dcr1Δ* cells caused a decrease in transcripts to a level similar to that of *med18Δ* cells.

III- vii-b. Mediator is required for efficient transcription in heterochromatin.

The accumulation of RNA in *dcr1Δ* cells and *med18Δ* cells could be explained by defects in RNA degradation by RNAi and/or the exosome [12, 16], or by an increase in heterochromatic transcription. To examine the latter possibility, localization of RNAPII at *cenH* and *kint2::ura4⁺* was examined by ChIP assay (Figure 13E). Unexpectedly, RNAPII was significantly increased in *dcr1Δ* cells at both loci in spite of the maintenance of heterochromatin in this strain, suggesting that Dcr1 negatively regulates heterochromatin transcription. Note that RNAi machinery has been shown to interact with RNAPII and modulate transcription in other organisms [42, 43]. Thus, an increase in transcription and prevention of processing of RNA into siRNA could cause the observed accumulation of transcripts in *dcr1Δ* cells

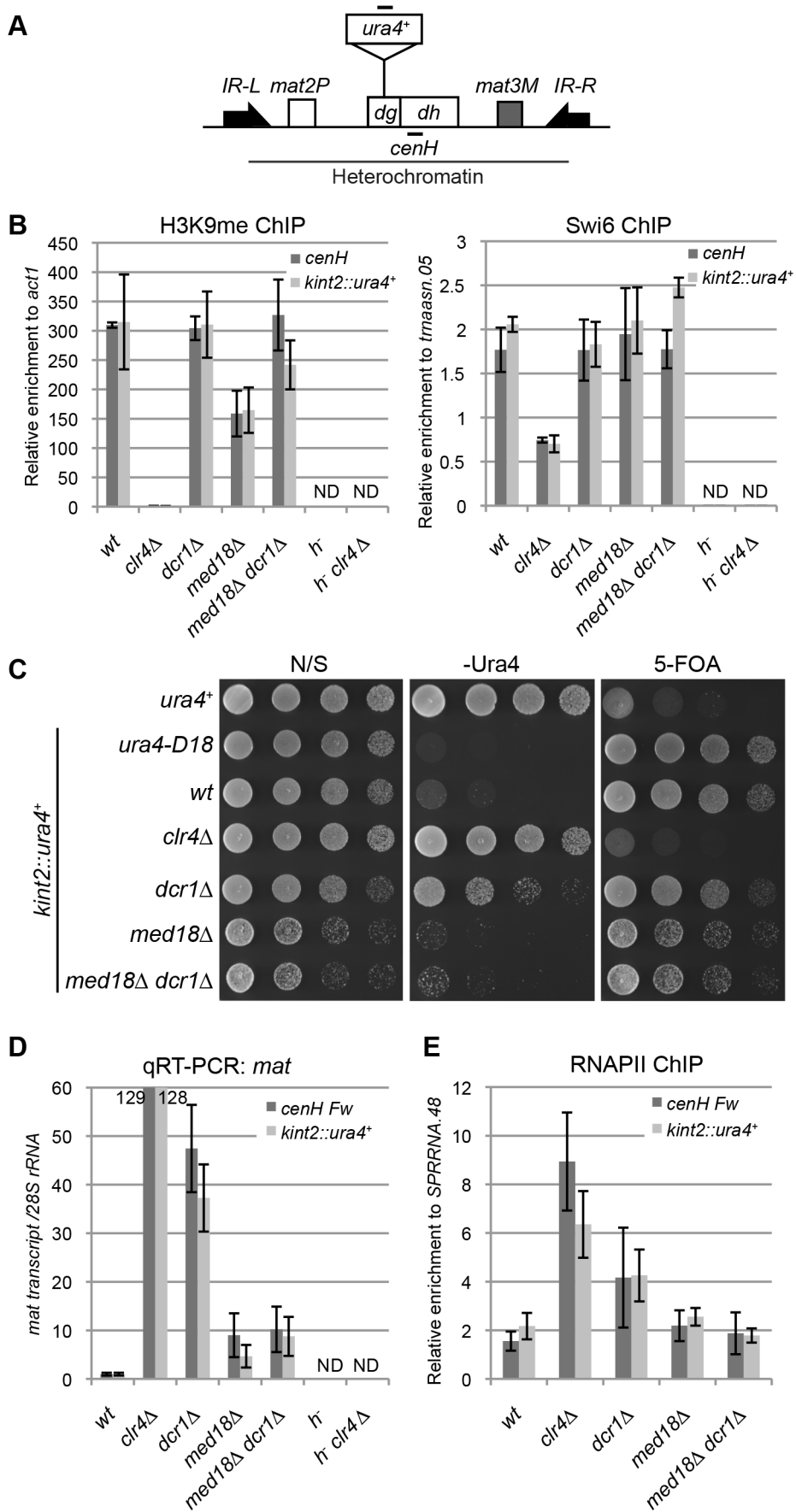


Figure 13. Mediator is required for transcriptional activation in heterochromatin

(A) Schematic of the fission yeast mating-type locus. Location of the *ura4* reporter inserted within the *cenH* is shown (*kint2::ura4*⁺). Black bars indicate the location of primers or probes used for ChIP, RT-PCR and northern analysis. (B) ChIP analysis of H3K9me2 and Swi6 at *cenH dh* repeats or *kint2::ura4*⁺, each relative to *act1* or *trnaasn.05*. Error bars show the standard error of the mean (n = 3). (C) Silencing assay at the mating-type locus. The results of serial dilutions of the indicated strains spotted onto N/S, 5-FOA media and medium without uracil (-URA) for the silencing of *ura4* are shown. Note that PMGS (EMMS-NH₄Cl (nitrogen), +L-glutamic acid, monosodium, as nitrogen) plates were used as N/S plates. (D) Quantitative RT-PCR analysis of *cenH dh* repeats or *kint2::ura4*⁺ forward transcript levels relative to a control *SPRRNA.48*, whose levels were normalized to that of the wild-type in the indicated strains. Error bars show the standard error of the mean (n = 3). (E) ChIP analysis of RNAPII at *cenH dh* repeats or *kint2::ura4*⁺ relative to *SPRRNA.48*. Error bars show the standard error of the mean (n = 3). P values were determined using a two-sided Student's t-test. Note that in Figures B, D and E, *h*⁻ strains (*h*⁻, *h clr4Δ*), which do not have *cenH* sequence, were included to show the primer used in the experiments detected only *cenH*

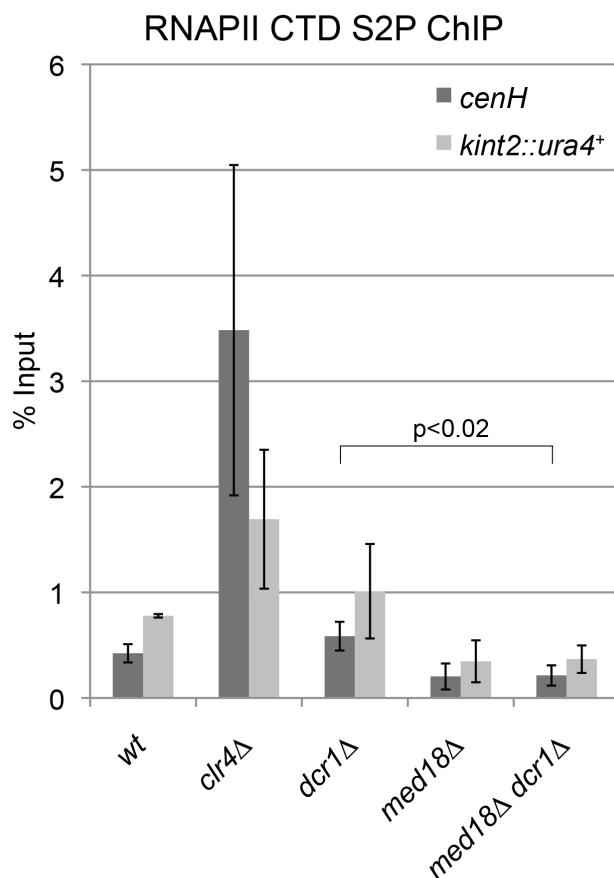


Figure 14. Mediator is required for transcriptional activation in heterochromatin.

ChIP analysis of RNAPII at *cenH dh* repeats or *kint2::ura4*⁺ relative to input WCE in the indicated strains. Anti-RNA polymerase II CTD serine 2 phosphorylation was used. Error bars represent the standard error of the mean (n = 3). P values were determined using a two-sided Student's t-test.

(Figure 13D). By contrast, the level of RNAPII in *med18* Δ cells was comparable to that of wild-type cells (Figure 13E). Similar results of RNAPII localization were obtained with ChIP assay using the antibody against RNAPII-C-terminal repeats phosphorylated at the second serine, which represents elongating RNAPII (Figure 14). This indicated that Med18 did not repress transcription in heterochromatin. The approximately 10-fold accumulation of *cenH* and *kint2::ura4⁺* RNA observed in *med18* Δ cells might be due to the prevention of exosome-dependent degradation of RNA [16], which would indicate that significant transcription took place in the absence of Med18. Importantly, introduction of *med18* Δ into *dcr1* Δ cells caused a decrease in RNAPII to the level of wild-type cells, suggesting that Mediator is required for efficient transcription in heterochromatin in *dcr1* Δ cells.

III- vii-c. Med18 negatively regulates transcription in the compromised heterochromatin.

To analyze the role of Med18 on the transcription in the absence of heterochromatin, we compared RNAPII occupancy at centromeric repeats of *dcr1* Δ *rrp6* Δ cells with those of *dcr1* Δ *rrp6* Δ *med18* Δ cells (Figure 15). Note that both strains showed similarly low levels of H3K9me at *dh* repeats (Figure 10C). Introduction of *med18* Δ caused the moderate increase of RNAPII. This suggested that Med18 negatively regulates transcription in the compromised heterochromatin.

III-vii-d. Conclusion

From these data, we suggest that Med18/Mediator does not negatively regulate pericentromeric transcription when heterochromatin is established; rather, it might be required for efficient transcription in heterochromatin.

III-viii. Effect of Mediator disruption on euchromatic genes

III-viii-a. The effect of *med18* Δ and *med20* Δ on euchromatic gene expression.

The effect of *med18* Δ and *med20* Δ on euchromatic gene expression was further examined using microarray. Pink and white epiclones of *med18* Δ and *med20* Δ cells were separated and the expression pattern of each epiclone was compared. Analysis of the genes that showed ≥ 1.5 -fold increase (Up) or decrease (Down) in

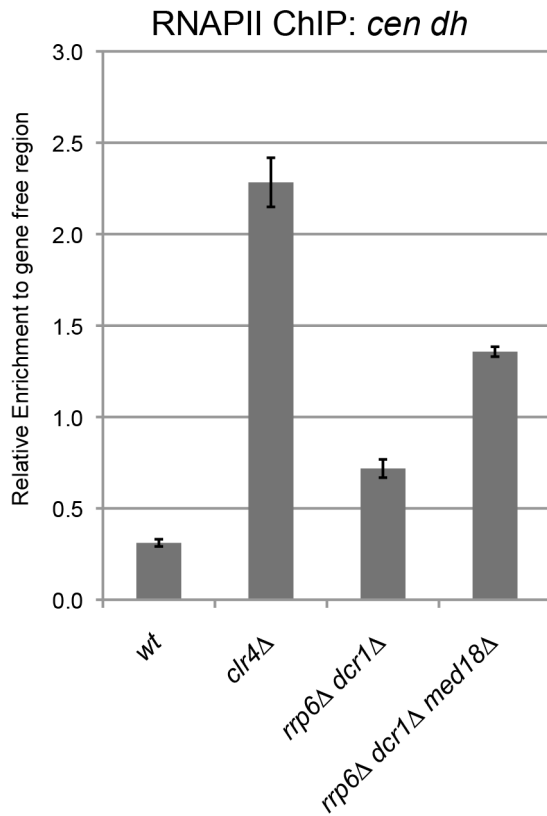


Figure 15. Mediator negatively regulates RNAPII in the compromised heterochromatin.

ChIP analysis of RNAPII at *dh* repeats relative to gene free region in the indicated strains.

Error bars show the standard error of the mean (n = 3).

expression between the epiclones revealed that a common set of genes were affected in both *med18Δ* cells and *med20Δ* cells, irrespective of the state of heterochromatic silencing (Figure 16A). Therefore, a clear difference between the white and pink epiclones was observed at pericentromeric ncRNA expression. Indeed, in the white epiclones, no euchromatic genes showed stronger induction than centromeric ncRNA; the most strongly increased euchromatic gene showed an approximately 14-fold and 26-fold increase in *med18Δ-w* and *med20Δ-w* cells, respectively, which is much weaker than the increase in centromeric ncRNA (which increased by more than 100-fold). Comparison of *med18Δ-w* and *med20Δ-w*, or *med18Δ-p* and *med20Δ-p*, showed that both subunits shared a common set of targets (Figure 17). This is consistent with the fact that both Med18 and Med20 formed heterodimers that consisted of a region of the head domain in Mediator.

III-viii-b. Some euchromatic genes, including stress response genes, might be repressed by the RNAi/Mediator system.

When the expression pattern of the Mediator mutants was compared with that of *dcr1Δ* cells, it was evident that the expression of a common set of genes was increased in both *med18Δ-w/med20Δ-w* cells and *dcr1Δ* cells (Figure 16B, upper panels). Similar sharing of target genes was observed between *med18Δ-p/med20Δ-p* cells and *dcr1Δ* cells (Figure 16B, lower panel). Interestingly, gene ontology analysis showed significant enrichment of terms pertaining to stress responses in the shared target genes. For example, the top GO terms included “cellular response to stimulus” (GO: 0033554, *med18Δ-w* vs. *dcr1Δ* $P = 5.35 \times 10^{-3}$, *med18Δ-p* vs. *dcr1Δ* $P = 2.2 \times 10^{-6}$, *med20Δ-w* vs. *dcr1Δ* $P = 2.19 \times 10^{-6}$, *med20Δ-p* vs. *dcr1Δ* $P = 1.27 \times 10^{-4}$). These results suggest that some euchromatic genes, including stress response genes, are repressed by the RNAi/Mediator system, which may function via a mechanism partly similar to that of RNAi-mediated heterochromatin.

III-viii-c. Conclusion

These data suggests that a common set of euchromatic genes were affected in both *med18Δ* cells and *med20Δ* cells, and some euchromatic genes, including stress response genes, are repressed by the RNAi/Mediator system.

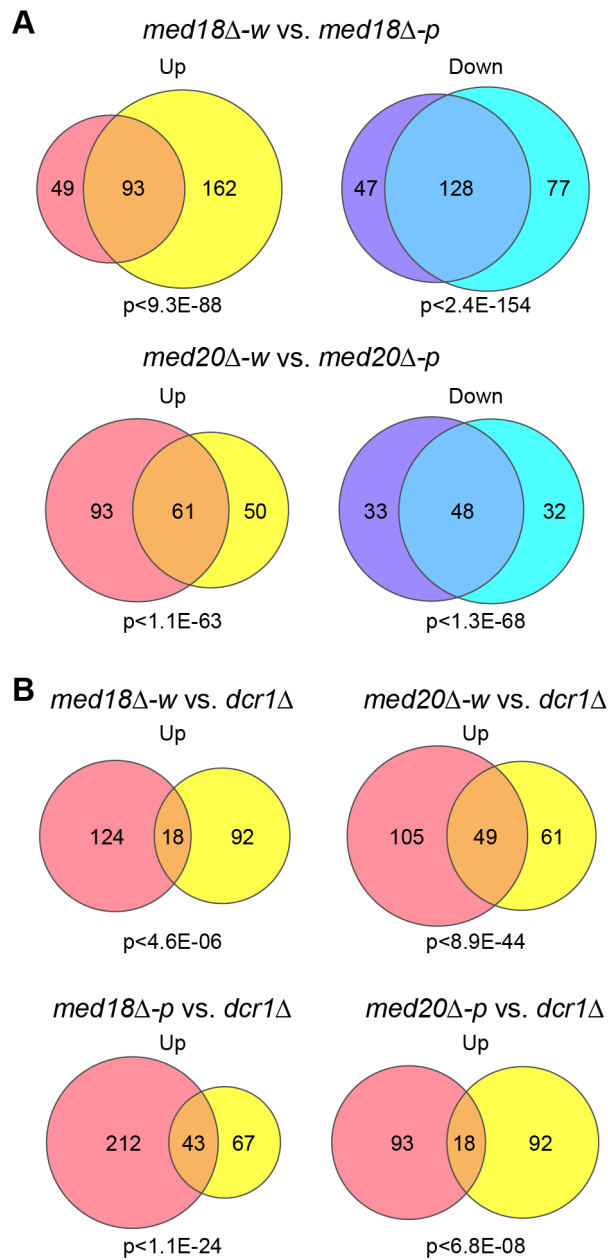


Figure 16. Effect of Mediator disruption on euchromatic genes

Venn diagram showing the number of transcripts whose expression levels are increased (up) or decreased (down) >1.5-fold in mutants compared to the wild-type. P-values were calculated using Fisher's exact test. (A) Transcripts of *med18Δ-w* (left circles) vs. *med18Δ-p* (right circles) mutants (top) and *med20Δ-w* (left circles) vs. *med20Δ-p* (right circles) mutants (bottom). (B) Transcripts of *med18Δ-w* (left circles) vs. *dcr1Δ* (right circles) mutants (upper left), *med20Δ-w* (left circles) vs. *dcr1Δ* (right circles) mutants (upper right), *med18Δ-p* (left circles) vs. *dcr1Δ* (right circles) mutants (lower left), and *med20Δ-p* (left circles) vs. *dcr1Δ* (right circles) mutants (lower right).

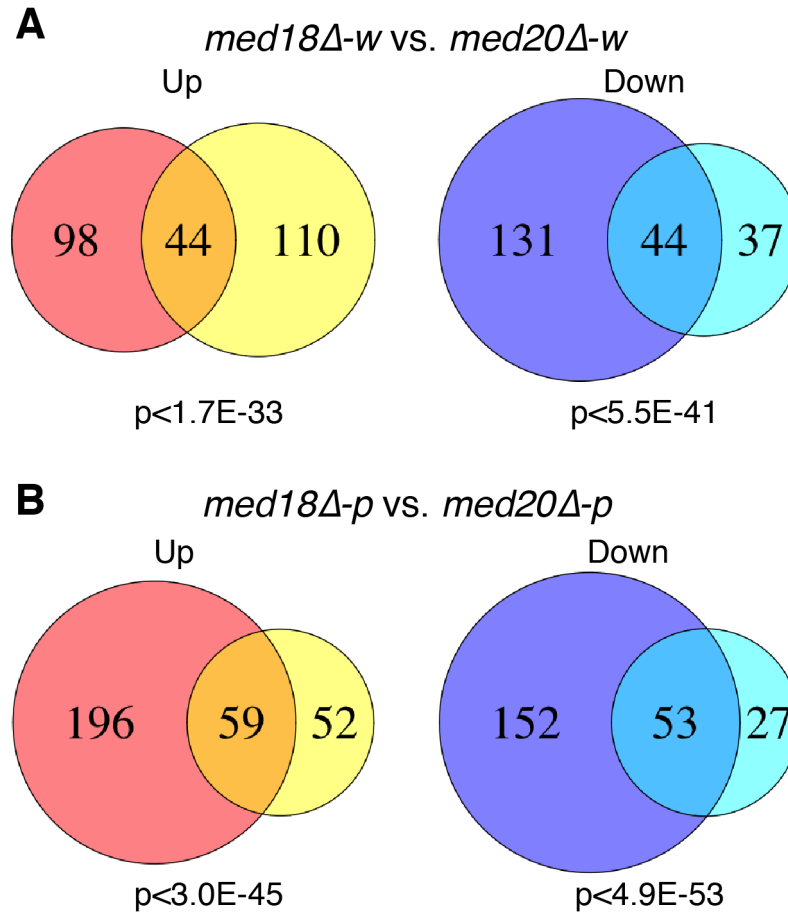


Figure 17. Effect of Mediator disruption on euchromatic genes

Venn diagram showing the number of transcripts whose the expression levels were increased (up) or decreased (down) >1.5-fold in mutants compared to the wild type. The p-value was calculated using Fisher's exact test. (A) Transcripts of *med18Δ-w* (left circles) vs. *med20Δ-w* (right circles) mutants. (B) Transcripts of *med18Δ-p* (left circles) vs. *med20Δ-p* (right circles) mutants.

IV. Discussion

In this study, we showed that the specific subunits of Mediator, Med18/Med18, Med20, Med8 and Med31 were involved in pericentromeric heterochromatin formation. The Med18/Med20 heterodimer is a component of the head domain of Mediator [24]. Because the *med8-K9* mutation causes truncation of the C-terminal domain that interacts with the Med18/Med20 heterodimer (Figure 5B), it resulted in the loss of the heterodimer formation. Importantly, Med31 belongs to the middle domain but is located close to the head domain [44], suggesting that the head domain does not function alone in heterochromatin formation, but rather as a part of Mediator. Therefore, we suggest that Mediator specifically plays multiple roles in the formation of pericentromeric heterochromatin via the Mediator head domain (MHD).

IV-i. Efficient siRNA production is required for effective spreading.

Two distinct mechanisms, the RNAi-dependent and Rrp6-dependent pathways, function in heterochromatin formation at pericentromeric repeats, while the spreading of H3K9me onto marker genes mainly depends on the RNAi pathway [14, 15]. We found that at the pericentromeric heterochromatin, the absence of MHD compromises the Rrp6-dependent pathway and H3K9me is largely maintained by the RNAi-dependent pathway (Fig. 10). The finding that the amount of siRNA produced in the white epiclones of MHD mutants decreased to 3–20% of that of wild-type cells (Fig. 11A and Figure 12A) indicates that only a small amount of siRNA is necessary to maintain heterochromatin at the pericentromeric repeats. The remaining H3K9me at the repeats in MHD mutants spreads onto the marker genes by an RNAi-dependent mechanism. This process was also compromised by the decrease of siRNA caused by the absence of MHD, resulting in variegation of the level of H3K9me at the marker genes, which ultimately caused the appearance of white and pink epiclones. The spreading process appears to require more efficient siRNA production than the maintenance of heterochromatin at the pericentromeric repeats because *med18Δ-p* cells that produced more siRNA showed more efficient spreading of H3K9me and silencing of marker genes than *med18Δ-w* cells. In contrast, *dcr1Δ* cells did not show the variegation of silencing because of loss of siRNA production. It is noteworthy that the variegated phenotype was metastable, which suggests that once

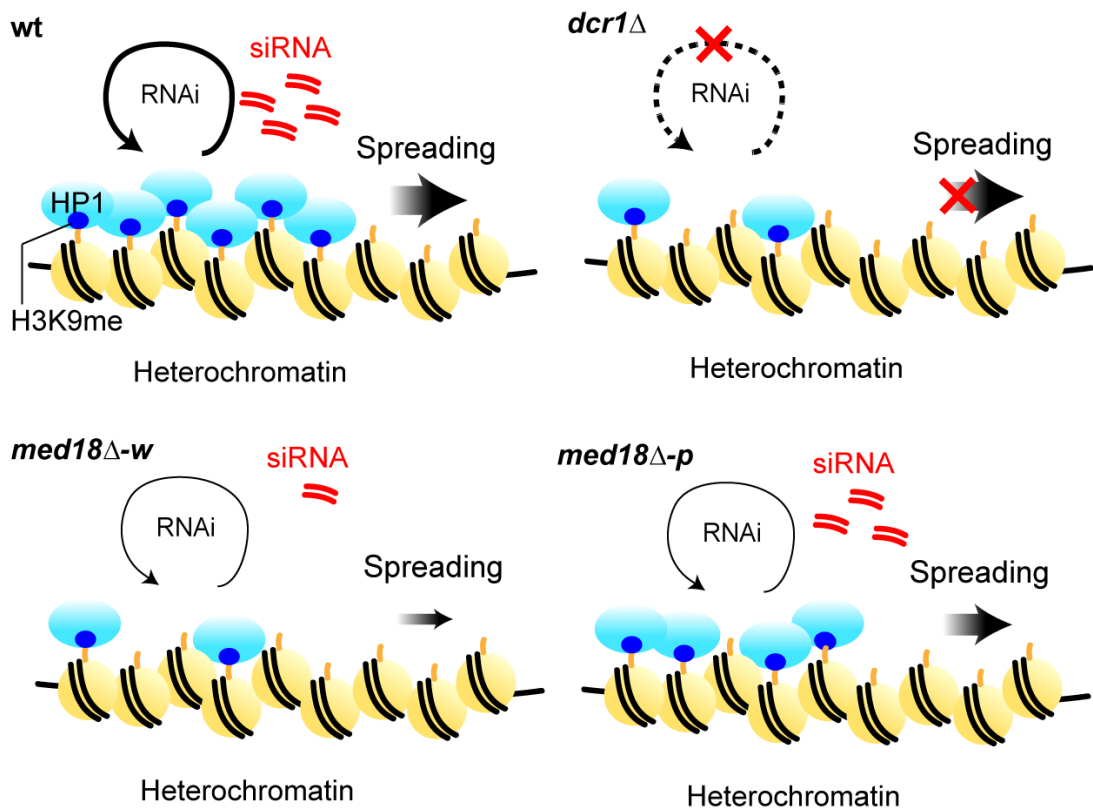


Figure 18. Efficient siRNA production is required for effective spreading

The spreading process appears to require more efficient siRNA production than the maintenance of heterochromatin at the pericentromeric repeats because *med18*Δ-*p* cells that produced more siRNA showed more efficient spreading of H3K9me and silencing of marker genes than *med18*Δ-*w* cells. In contrast, *dcr1*Δ cells did not show the variegation of silencing because of loss of siRNA production. It is noteworthy that the variegated phenotype was metastable, which suggests that once heterochromatin was spread into the marker gene, it could be maintained in an MHD-independent manner, probably through the small amount of siRNA produced in MHD mutants

heterochromatin was spread into the marker gene, it could be maintained in an MHD-independent manner, probably through the small amount of siRNA produced in MHD mutants (Figure 18).

IV-ii. MHD functions after RITS associates with heterochromatic repeats and/or target RNA.

Many processes involved in RNA processing, such as RNA splicing and RNA transport, are coupled to transcription by RNAPII. siRNA production is also coupled with RNAPII-dependent transcription [10]. Our results showed that the mutation of MHD resulted in a large decrease in siRNA. By contrast, *rrp6* Δ cells, which have levels of H3K9me and Swi6 at the pericentromeric repeats similar to *med18* Δ cells (Fig. 10), produced the same amount of siRNA as wild-type cells [16]. These results indicate that MHD is somehow involved in siRNA production after transcription of ncRNA. MHD is localized at the transcribed region in pericentromeric repeats (Figure 8; [39, 40] and is required for transcription in heterochromatin, suggesting that it directly functions in the coupling of transcription of heterochromatic ncRNA by RNAPII and processing of the siRNA by RNAi machinery. Retention of RNAi factors at the pericentromeric repeats in *med18* Δ cells and the requirement for MHD in heterochromatin formation via the artificial tethering of the RITS complex to RNA suggest that MHD functions after RITS associates with heterochromatic repeats and/or target RNA. Recently, we showed that RNAi factors are assembled into an siRNA amplification compartment that includes transcriptionally active heterochromatin [45]. Thus, MHD might be involved in the formation of this compartment. Although we were not able to detect a stable interaction between MHD components and RNAi factors, such as Ago1, by co-immunoprecipitation experiments (data not shown), it is still possible that MHD recruits factors required for siRNA generation to transcriptionally active heterochromatin through direct or indirect interactions. In any case, further experiments are necessary to clarify the molecular function of Mediator in the RNAi pathway (Figure 19).

IV-iii. Mediator acts in a step after the association of Rrp6/exosome with chromatin.

In contrast to the RNAi pathway, little is known about the Rrp6-dependent heterochromatin formation pathway. As deletion of *rrp6* marginally affects H3K9me

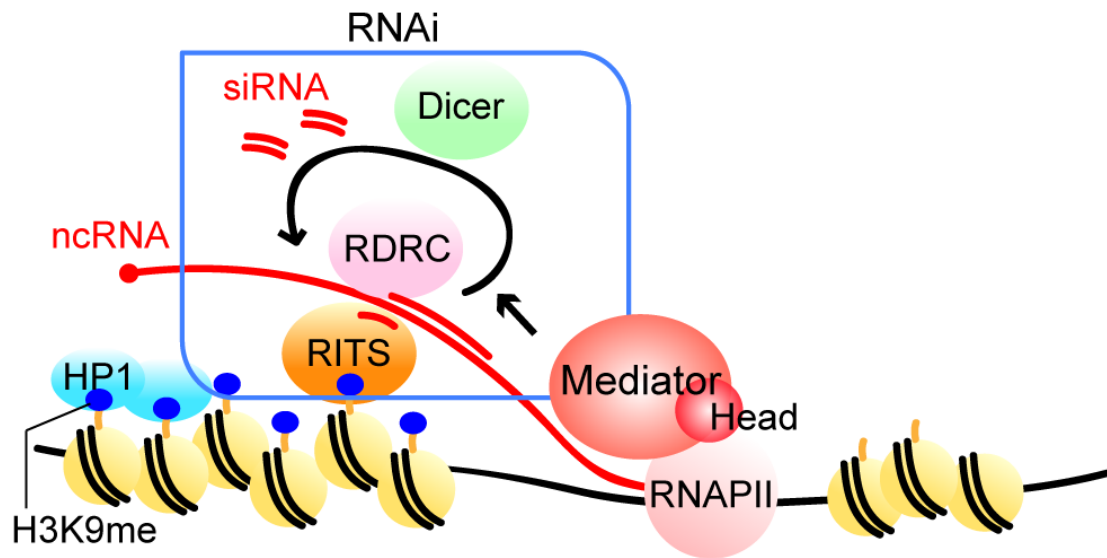


Figure 19. MHD functions after RITS associates with heterochromatic repeats and/or target RNA.

Retention of RNAi factors at the pericentromeric repeats in *med18Δ* cells and the requirement for MHD in heterochromatin formation via the artificial tethering of the RITS complex to RNA suggest that MHD functions after RITS associates with heterochromatic repeats and/or target RNA.

and silencing at the inserted marker genes [16, 18], the Rrp6-dependent pathway mainly functions at the pericentromeric repeats. Our genetic experiments showed that *rrp6* and *med18* were epistatic in the formation of pericentromeric heterochromatin (Fig. 10), indicating that MHD functions in Rrp6-dependent heterochromatin formation. Rrp6 is an exonuclease that is a subunit of the nuclear exosome involved in RNA-quality control [46]. A functional relationship between Mediator and the nuclear exosome has not been reported. We found that Rrp6 associates with both heterochromatin (*dh*) and euchromatin (*act1* and *fbp1*) and deletion of *med18* did not affect the localization, suggesting Mediator acts in a step after the association of Rrp6/exosome with chromatin. This is analogous to the function of Mediator in the RNAi-dependent pathway that MHD functions after recruitment of RITS complex and RDRC to chromatin. Considering the co-transcriptional nature of RNA-quality control [47, 48] and recruitment of RNA-splicing factors to transcripts by Mediator [27], we speculate that MHD plays a role in the co-transcriptional function of chromatin-associated Rrp6 and/or other co-factors to promote heterochromatin formation. Alternatively, given that the RNAi-independent heterochromatin nucleation pathway and Mediator functionally interact with RNAPII processivity factors [18, 28], Mediator may promote Rrp6-dependent heterochromatin formation by affecting elongation by RNAPII through interaction with these processivity factors. It is also possible that the same mechanism is also involved in RNAi-dependent heterochromatin formation through MHD (Figure 20).

IV-iv. Mediator is required for transcriptional activation in heterochromatin.

Recently, two reports showed that MHD was important for heterochromatin formation at pericentromeres [39, 40]. However, there are several discrepancies between their data and ours. Firstly, the decrease in H3K9me and Swi6 in *med20Δ* cells was much more severe than that than in ours. Secondly, Carlsten et al. claimed that siRNA from the *dh* repeat in *med20Δ* cells was diminished but that siRNA from the *dg* repeats was comparable to that in wild-type cells. Thirdly, both papers assert that Mediator negatively regulates heterochromatic transcription. The first two discrepancies could be caused by the variegated phenotype of MHD mutants. If this variegated phenotype was overlooked or disregarded, the results would be affected by which epiclones were used in the experiments. In addition, since the amount of

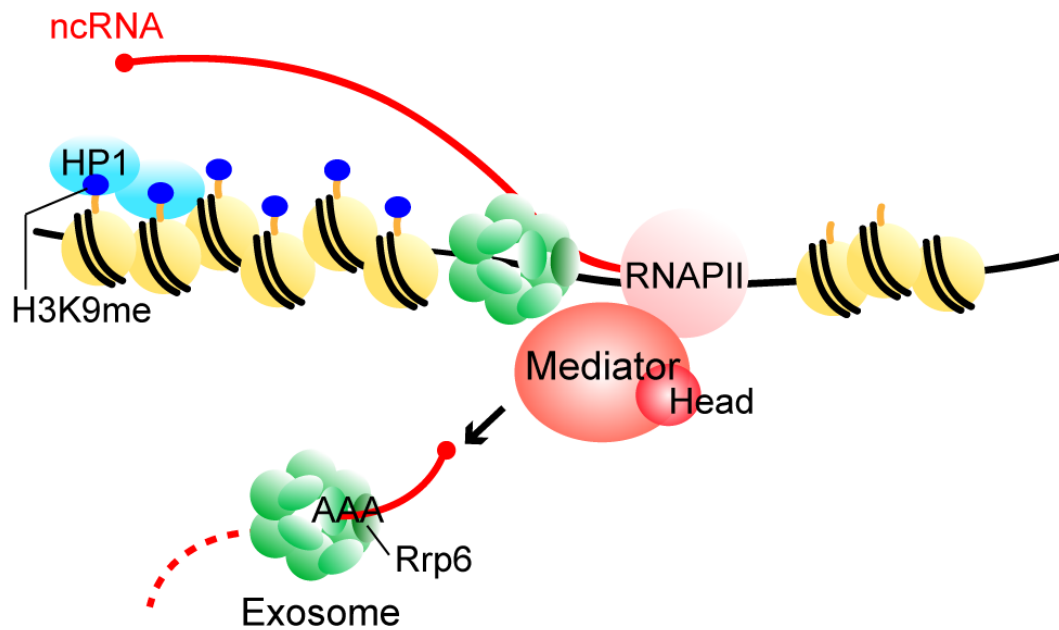


Figure 20. Mediator acts in a step after the association of Rrp6/exosome with chromatin.

Considering the co-transcriptional nature of RNA-quality control and recruitment of RNA-splicing factors to transcripts by Mediator, we speculate that MHD plays a role in the co-transcriptional function of chromatin-associated Rrp6 and/or other co-factors to promote heterochromatin formation.

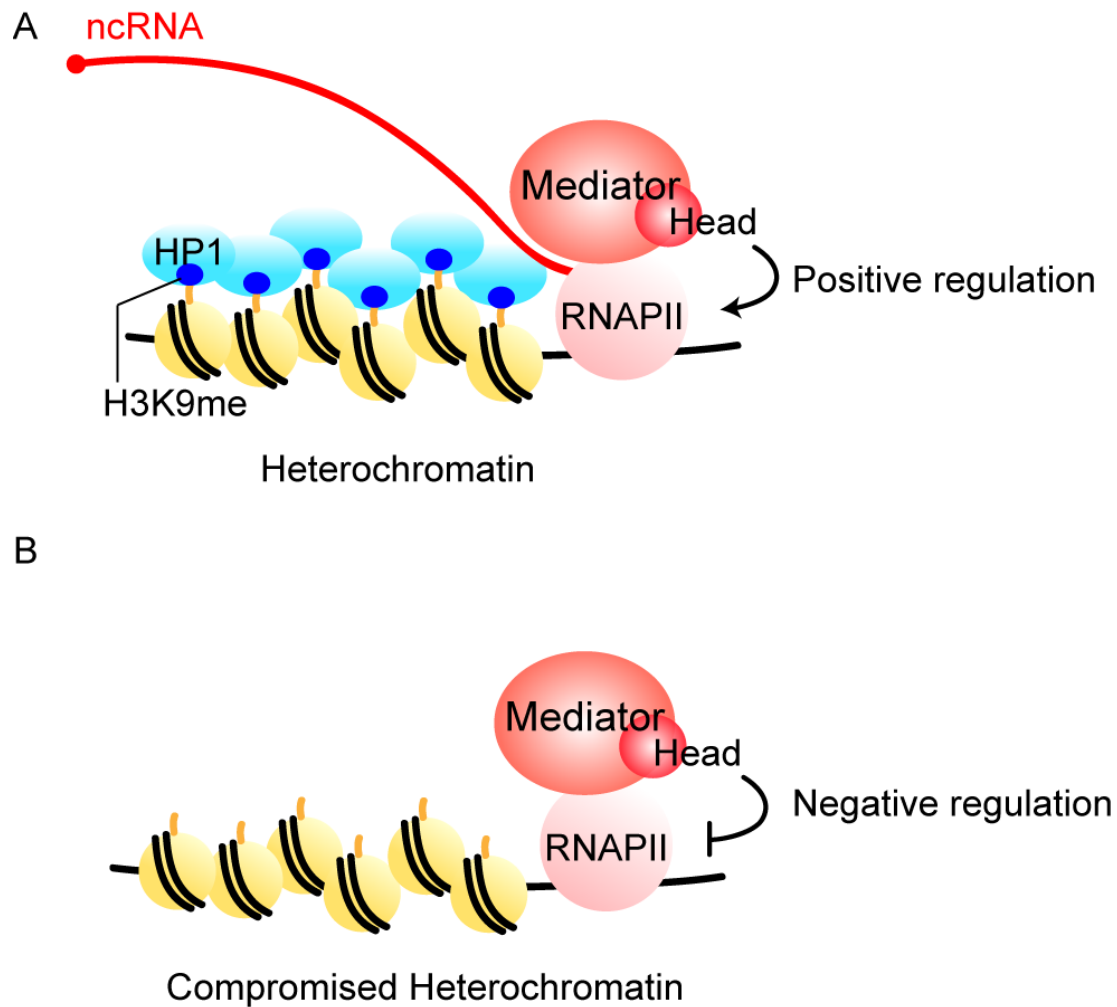


Figure 21. Mediator is required for transcriptional activation in heterochromatin.

Our data using mating locus heterochromatin showed that disruption of Mediator did not cause increased transcription in heterochromatin, rather it caused a decrease in transcription enhanced by deletion of *dcr1(A)*. Interestingly, when heterochromatin was compromised, Mediator appears to negatively regulate transcription, which might also explain the discrepancy (B).

H3K9me/Swi6 varies depending on the position in the repeats, the discrepancies between their results and ours might reflect a difference in the sites used for ChIP analysis. The third discrepancy could be explained by the use of pericentromeric transcription for their analysis. As described in the Results section, it is hard to argue definitively for the direct influence of MHD mutants on transcription in pericentromeric heterochromatin because it is difficult to determine whether the observed increase is due to the direct effect of depletion of MHD or a secondary effect resulting from the disruption of heterochromatin. Our data using mating locus heterochromatin showed that disruption of Mediator did not cause increased transcription in heterochromatin, rather it caused a decrease in transcription enhanced by deletion of *dcr1* (Fig. 13). Interestingly, when heterochromatin was compromised, Mediator appears to negatively regulate transcription, which might also explain the discrepancy (Figure 21).

IV-v. MHD functions in co-transcriptional degradation of euchromatic RNAs in collaboration with Dcr1.

Recently, Dcr1 was shown to repress a set of genes, including stress response genes, through the degradation of target RNA [49]. We identified a similar set of euchromatic genes that were up-regulated in *med20Δ* and *dcr1Δ* cells, suggesting that MHD functions in co-transcriptional degradation of euchromatic RNAs in collaboration with Dcr1. Note that previous transcriptome analysis of the mediator mutants also showed that a similar set of genes were up regulated in *med20Δ*, *med18Δ* cells but not in *med12Δ* cells, supporting the collaborative function of MHD and Dcr1 [50]. In addition, Rrp6-dependent heterochromatin formation was observed at several meiotic genes [51]. Moreover, the exosome and RNAi are shown to regulate a set of genes, including retrotransposons and developmental genes [52]. Therefore, it is also possible that Mediator functions at these loci to silence genes by regulating both RNAi and exosomal machineries.

IV-vi. Conclusion

We suggest that Mediator specifically plays multiple roles in the formation of pericentromeric heterochromatin via the Mediator head domain (MHD). Mediator is required for both siRNA formation in RNAi-dependent pathway and Rrp6-dependent

H3K9 methylation in pericentromeric heterochromatin. Moreover, Mediator also required for transcriptional activation in heterochromatin, whereas Mediator negatively regulates RNAPII in the compromised heterochromatin.

Emerging evidence shows that Mediator works as a platform for various factors that function in transcription and RNA processing, using a distinct subunit for particular interactions with the factors [27, 28]. Our results further extend the range of Mediator function to include regulation of higher-order chromatin structure in the genome. It is now widely accepted that RNAPII transcribes almost all of the genome. Mediator might not only mediate transcription factors and RNAPII at each gene, but also mediate RNAPII and genome-wide regulation of higher-order chromatin structure (Figure 22).

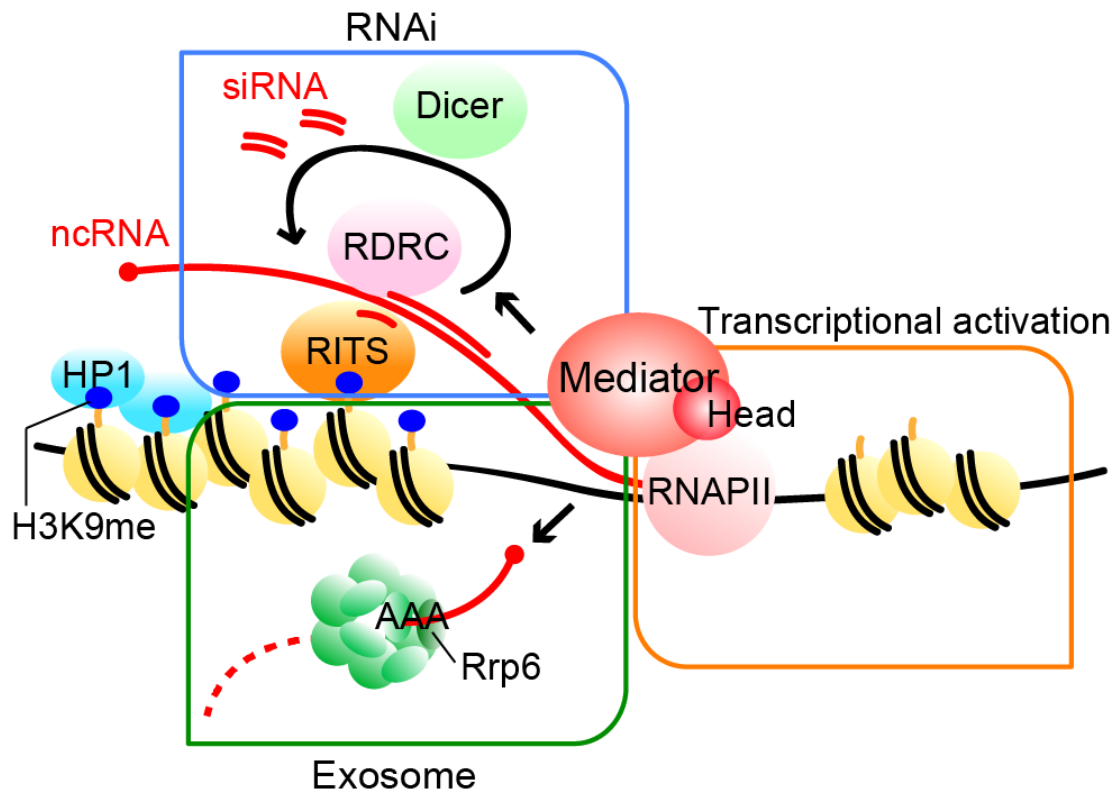


Figure 22. Model of the function of Mediator in pericentromeric heterochromatin assembly in fission yeast.

Mediator localizes to pericentromeres to recruit RNAPII for efficient transcription. Furthermore, Mediator regulates processing of transcribed ncRNA by RNAi machineries, which directs heterochromatin formation. In addition, Mediator is also required for Rrp6-dependent heterochromatin formation. For details, see Discussion.

V. Reference

1. Rea, S., et al., *Regulation of chromatin structure by site-specific histone H3 methyltransferases*. Nature, 2000. **406**(6796): p. 593-9.
2. Nakayama, J., et al., *Role of histone H3 lysine 9 methylation in epigenetic control of heterochromatin assembly*. Science, 2001. **292**(5514): p. 110-3.
3. Cam, H.P., et al., *Comprehensive analysis of heterochromatin- and RNAi-mediated epigenetic control of the fission yeast genome*. Nat Genet, 2005. **37**(8): p. 809-19.
4. Grewal, S.I. and S. Jia, *Heterochromatin revisited*. Nat Rev Genet, 2007. **8**(1): p. 35-46.
5. Shimada, A. and Y. Murakami, *Dynamic regulation of heterochromatin function via phosphorylation of HP1-family proteins*. Epigenetics, 2010. **5**(1): p. 30-3.
6. Volpe, T.A., et al., *Regulation of heterochromatic silencing and histone H3 lysine-9 methylation by RNAi*. Science, 2002. **297**(5588): p. 1833-7.
7. Motamedi, M.R., et al., *Two RNAi complexes, RITS and RDRC, physically interact and localize to noncoding centromeric RNAs*. Cell, 2004. **119**(6): p. 789-802.
8. Chikashige, Y., et al., *Composite motifs and repeat symmetry in S. pombe centromeres: direct analysis by integration of NotI restriction sites*. Cell, 1989. **57**(5): p. 739-51.
9. Djupedal, I., et al., *RNA Pol II subunit Rpb7 promotes centromeric transcription and RNAi-directed chromatin silencing*. Genes Dev, 2005. **19**(19): p. 2301-6.
10. Kato, H., et al., *RNA polymerase II is required for RNAi-dependent heterochromatin assembly*. Science, 2005. **309**(5733): p. 467-9.
11. Chen, E.S., et al., *Cell cycle control of centromeric repeat transcription and heterochromatin assembly*. Nature, 2008. **451**(7179): p. 734-7.
12. Noma, K., et al., *RITS acts in cis to promote RNA interference-mediated transcriptional and post-transcriptional silencing*. Nat Genet, 2004. **36**(11): p. 1174-80.

13. Sugiyama, T., et al., *RNA-dependent RNA polymerase is an essential component of a self-enforcing loop coupling heterochromatin assembly to siRNA production*. Proc Natl Acad Sci U S A, 2005. **102**(1): p. 152-7.
14. Irvine, D.V., et al., *Argonaute slicing is required for heterochromatic silencing and spreading*. Science, 2006. **313**(5790): p. 1134-7.
15. Li, H., et al., *An alpha motif at Tas3 C terminus mediates RITS cis spreading and promotes heterochromatic gene silencing*. Mol Cell, 2009. **34**(2): p. 155-67.
16. Buhler, M., et al., *RNAi-dependent and -independent RNA turnover mechanisms contribute to heterochromatic gene silencing*. Cell, 2007. **129**(4): p. 707-21.
17. Buhler, M., et al., *TRAMP-mediated RNA surveillance prevents spurious entry of RNAs into the Schizosaccharomyces pombe siRNA pathway*. Nat Struct Mol Biol, 2008. **15**(10): p. 1015-23.
18. Reyes-Turcu, F.E., et al., *Defects in RNA quality control factors reveal RNAi-independent nucleation of heterochromatin*. Nat Struct Mol Biol, 2011. **18**(10): p. 1132-8.
19. Kelleher, R.J., 3rd, P.M. Flanagan, and R.D. Kornberg, *A novel mediator between activator proteins and the RNA polymerase II transcription apparatus*. Cell, 1990. **61**(7): p. 1209-15.
20. Kim, Y.J., et al., *A multiprotein mediator of transcriptional activation and its interaction with the C-terminal repeat domain of RNA polymerase II*. Cell, 1994. **77**(4): p. 599-608.
21. Soutourina, J., et al., *Direct interaction of RNA polymerase II and mediator required for transcription in vivo*. Science, 2011. **331**(6023): p. 1451-4.
22. Lariviere, L., M. Seizl, and P. Cramer, *A structural perspective on Mediator function*. Curr Opin Cell Biol, 2012. **24**(3): p. 305-13.
23. Bourbon, H.M., *Comparative genomics supports a deep evolutionary origin for the large, four-module transcriptional mediator complex*. Nucleic Acids Res, 2008. **36**(12): p. 3993-4008.
24. Lariviere, L., et al., *Structure and TBP binding of the Mediator head subcomplex Med8-Med18-Med20*. Nat Struct Mol Biol, 2006. **13**(10): p. 895-901.

25. Imasaki, T., et al., *Architecture of the Mediator head module*. Nature, 2011. **475**(7355): p. 240-3.
26. Kim, Y.J., et al., *The role of Mediator in small and long noncoding RNA production in Arabidopsis thaliana*. EMBO J, 2011. **30**(5): p. 814-22.
27. Huang, Y., et al., *Mediator complex regulates alternative mRNA processing via the MED23 subunit*. Mol Cell, 2012. **45**(4): p. 459-69.
28. Takahashi, H., et al., *Human mediator subunit MED26 functions as a docking site for transcription elongation factors*. Cell, 2011. **146**(1): p. 92-104.
29. Xhemalce, B. and T. Kouzarides, *A chromodomain switch mediated by histone H3 Lys 4 acetylation regulates heterochromatin assembly*. Genes Dev, 2010. **24**(7): p. 647-52.
30. Bahler, J., et al., *Heterologous modules for efficient and versatile PCR-based gene targeting in Schizosaccharomyces pombe*. Yeast, 1998. **14**(10): p. 943-51.
31. Schmitt, M.E., T.A. Brown, and B.L. Trumpower, *A rapid and simple method for preparation of RNA from Saccharomyces cerevisiae*. Nucleic Acids Res, 1990. **18**(10): p. 3091-2.
32. Tange, Y., et al., *The CCR4-NOT complex is implicated in the viability of aneuploid yeasts*. PLoS Genet, 2012. **8**(6): p. e1002776.
33. Nakagawa, H., et al., *Fission yeast CENP-B homologs nucleate centromeric heterochromatin by promoting heterochromatin-specific histone tail modifications*. Genes Dev, 2002. **16**(14): p. 1766-78.
34. Kipling, D. and S.E. Kearsey, *Reversion of autonomously replicating sequence mutations in Saccharomyces cerevisiae: creation of a eucaryotic replication origin within procaryotic vector DNA*. Mol Cell Biol, 1990. **10**(1): p. 265-72.
35. Allshire, R.C., et al., *Mutations derepressing silent centromeric domains in fission yeast disrupt chromosome segregation*. Genes Dev, 1995. **9**(2): p. 218-233.
36. Guglielmi, B., et al., *A high resolution protein interaction map of the yeast Mediator complex*. Nucleic Acids Res, 2004. **32**(18): p. 5379-91.
37. Verdel, A., et al., *RNAi-mediated targeting of heterochromatin by the RITS complex*. Science, 2004. **303**(5658): p. 672-6.

38. Buhler, M., A. Verdel, and D. Moazed, *Tethering RITS to a nascent transcript initiates RNAi- and heterochromatin-dependent gene silencing*. *Cell*, 2006. **125**(5): p. 873-86.
39. Carlsten, J.O., et al., *Mediator Promotes CENP-A Incorporation at Fission Yeast Centromeres*. *Mol Cell Biol*, 2012.
40. Thorsen, M., et al., *Mediator regulates non-coding RNA transcription at fission yeast centromeres*. *Epigenetics Chromatin*, 2012. **5**(1): p. 19.
41. Jia, S., K. Noma, and S.I. Grewal, *RNAi-independent heterochromatin nucleation by the stress-activated ATF/CREB family proteins*. *Science*, 2004. **304**(5679): p. 1971-6.
42. Kavi, H.H. and J.A. Birchler, *Interaction of RNA polymerase II and the small RNA machinery affects heterochromatic silencing in Drosophila*. *Epigenetics Chromatin*, 2009. **2**(1): p. 15.
43. Guang, S., et al., *Small regulatory RNAs inhibit RNA polymerase II during the elongation phase of transcription*. *Nature*, 2010. **465**(7301): p. 1097-101.
44. Cai, G., et al., *Mediator head module structure and functional interactions*. *Nat Struct Mol Biol*, 2010. **17**(3): p. 273-9.
45. Kawakami, K., et al., *A novel RNAi protein, Dsh1, assembles RNAi machinery on chromatin to amplify heterochromatic siRNA*. *Genes Dev*, 2012. **26**(16): p. 1811-24.
46. Houseley, J., J. LaCava, and D. Tollervey, *RNA-quality control by the exosome*. *Nat Rev Mol Cell Biol*, 2006. **7**(7): p. 529-39.
47. Huertas, P. and A. Aguilera, *Cotranscriptionally formed DNA:RNA hybrids mediate transcription elongation impairment and transcription-associated recombination*. *Mol Cell*, 2003. **12**(3): p. 711-21.
48. Suganuma, N., et al., *The Lotus japonicus Sen1 gene controls rhizobial differentiation into nitrogen-fixing bacteroids in nodules*. *Mol Genet Genomics*, 2003. **269**(3): p. 312-20.
49. Woolcock, K.J., et al., *RNAi keeps Atf1-bound stress response genes in check at nuclear pores*. *Genes Dev*, 2012. **26**(7): p. 683-92.
50. Linder, T., et al., *Two conserved modules of Schizosaccharomyces pombe Mediator regulate distinct cellular pathways*. *Nucleic Acids Res*, 2008. **36**(8): p. 2489-504.

51. Zofall, M., et al., *RNA elimination machinery targeting meiotic mRNAs promotes facultative heterochromatin formation*. *Science*, 2012. **335**(6064): p. 96-100.
52. Yamanaka, S., et al., *RNAi triggered by specialized machinery silences developmental genes and retrotransposons*. *Nature*, 2012.

VI. Acknowledgement

I would like to express my sincere gratitude to Professor Yota Murakami of Hokkaido University for his support and encouragement throughout the research.

I would like to express my gratitude to Professor Koji Ishimori and Kazuyasu Sakaguchi of Hokkaido University for accepting the vice-chairman of my doctoral dissertation.

I would like to express my gratitude to laboratory members, especially Associate Professor Masayuki Takahashi, Assistant Professor Shinya Takahata, Akiko Nakatomi of Hokkaido University for helpful discussion and support.

I would like to thank D. Moazed, S. Grewal and R. Allshire for the strains, T. Urano for the H3K9me antibody, and D.B. Goto for technical advice about small RNA analysis.

I would like to express my gratitude to Assistant Professor Hiroaki Kato of Shimane University for his support and encouragement.

I would like to express my gratitude to Associate Professor Jun-ichi Nakayama of Nagoya City University for his support and encouragement.

Finally, I would like to express my gratitude to my family and friends for their support and encouragement.